Published in final edited form as:
Hear Res. 2008 December ; 246(1-2): 59–78. doi:10.1016/j.heares.2008.09.010.

Acute Changes in Frequency Responses of Inferior Colliculus Central Nucleus (ICC) Neurons Following Progressively Enlarged Restricted Spiral Ganglion Lesions

Russell L. Snyder[1,2], **Ben H. Bonham**[1], and **Donal G. Sinex**[2]

1 *Department of Otolaryngology University of California, San Francisco, CA 94143-0526*

2 *Department of Psychology, Utah State University, Logan UT 84322-2810*

Abstract

Immediate effects of sequential and progressively enlarged spiral ganglion (SG) lesions were recorded from cochleas and inferior colliculi. Small SG-lesions produced modest elevations in cochlear tone-evoked compound action potential (CAP) thresholds across narrow frequency ranges; progressively enlarged lesions produced progressively higher CAP-threshold elevations across progressively wider frequency ranges. No comparable changes in distortion product otoacoustic emissions (DPOAEs) amplitudes were observed consistent with silencing of auditory nerve sectors without affecting organ of Corti function.

Frequency response areas (FRAs) of inferior colliculus (IC) neurons were recorded before and immediately after SG-lesions using multi-site silicon arrays fixed in place with recording sites arrayed along IC frequency gradient. Individual post-lesion FRAs exhibited progressively elevated response thresholds and diminished response amplitudes at lesion frequencies, whereas responses at non-lesion frequencies were either unchanged or enhanced. Characteristic frequencies were shifted and silent areas were introduced within these FRAs. Sequentially larger lesions produced sequentially larger shifts in CF and/or enlarged silent areas within affected FRAs, producing immediate changes in IC frequency organization.

These results contrast with those from the auditory nerve, extend previous reports of experience-induced plasticity in the auditory CNS, and support results indicating afferent convergence onto ICC neurons across broad frequency bands.

Keywords

Plasticity; inferior colliculus; hearing loss; tonotopic reorganization; cochleotopic organization; cochlear lesions; auditory; tonotopy

Send correspondence to: Russell L. Snyder, Ph.D., Epstein Laboratory, Box 0526, U490, University of California, San Francisco, CA 94143-0526, Tel: 415/476-1726, Fax: 415/476-2169, rsnyder@ohns.ucsf.edu.

INTRODUCTION

In the auditory system the topographic representation of tone frequency, or tonotopy, is a ubiquitous and thoroughly documented organizational principle. In the periphery inner hair cells are tonotopically organized and each inner hair cell has tonotopic connections through to cells in the cochlear nucleus via its associated spiral ganglion cells (Cant and Morest, 1984 for review). In the central auditory system, however, tonotopy coexists with extensive convergent projections across frequency channels at all levels (see Ehret, 1997 for review). These convergent projections along with the extensive spread of dendritic processes of neurons across the tonotopic projections within central auditory areas (e.g., see Rhode, 1991) make "labeled-line" mechanisms of tonotopy unlikely.

Moreover, if central tonotopy is based on labeled-line relays, these relays must be highly plastic, since tonotopy has been shown to be plastic on a scale that is inconsistent with fixed labeled-lines. For example, it has long been known that in young mammals, prior to the onset of hearing, chronic alterations in cochlear output produce functional and structural changes in central auditory organization (see Kitzes, 1996; Tierney et al., 1997 for review). More recently in adults, however, chronic alterations in cochlear output in the form of focal damage to the basilar membrane have been shown to produce changes in cortical tonotopy (see reviews by Weinberger, 1995, Palmer et al., 1998, Syka, 2003). Although these changes have been most thoroughly documented in primary auditory cortex, they have also been shown in inferior colliculus and cochlear nucleus by comparing tonotopy in normal animals with that in animals with chronic cochlear lesions (see Frisina and Rajan, 2005 for review).

Studies of tonotopic plasticity have described expanded representations of lesion-edge frequencies across post-lesion neural populations. These expanded lesion-edge frequency representations were presumed to occur within areas devoted to lesion frequencies prior to the lesions (e.g. see Robertson and Irvine, 1989; Rajan et al., 1993, 1998b, Eggermont and Komiya, 2000). However, some of these studies have reported expanded frequency representations that were also associated with elevations in threshold, and have been attributed directly to losses in peripheral sensitivity among single auditory nerve fibers. Therefore, they could not be attributed to central auditory plasticity, and have been termed "pseudoplasticity" (Kaltenbach et al., 1992,) or "residual" responses (Robertson and Irvine, 1989; Rajan et al., 1993, Rajan and Irvine, 1998a, b). Nevertheless, some *chronic* studies have revealed expansions of *cortical* representations of lesion-edge frequencies in adults without consistent elevations in minimum threshold indicating plastic changes in tuning of central auditory neurons that were inconsistent with the simple relay of peripheral lesion-induced changes. (e.g., Robertson and Irvine, 1989; Rajan et al., 1993; Willott et al., 1994; Rajan and Irvine, 1998a; Eggermont and Komiya, 2000, Norena et al., 2003).

Thus these cortical lesion-induced changes have been interpreted as indicative of experience dependent plasticity, which are specific to central auditory neurons. Alternatively, they could reflect immediate alterations in the frequency-specific balance between excitatory and inhibitory inputs onto central auditory neurons that persist chronically (Calford et al., 1993; Wang et al., 1996, Salvi et al., 1996; Kimura and Eggermont, 1999; Norena et al., 2003),. Therefore, although chronic studies illustrate the long term effects of peripheral lesions on central tonotopy, they give us little insight into the time course of these changes. Moreover, most of these chronic studies have examined changes in auditory cortex, and so do not distinguish between cortical and subcortical mechanisms.

In previous studies, we demonstrated that acute spiral ganglion lesions produced immediate changes in the frequency response properties of neurons in the central nucleus of the inferior colliculus (ICC) and that these changes altered the tonotopic organization of the ICC (Snyder

et al., 2000, Snyder and Sinex, 2002). We recorded frequency response areas (FRAs) of neurons distributed across the frequency organization using tungsten microelectrodes in map/re-map or fixed electrode paradigms. Both of these paradigms have limitations. For example, in the map/re-map studies (Snyder et al 2000) neural responses prior to the lesion are compared to responses of similar (but not identical) neurons after the lesions. In fixed tungsten electrode studies (Snyder and Sinex, 2002), microelectrodes were inserted and fixed at ICC locations prior to the lesion. Responses from the same neurons were recorded before and immediately after single SG lesion. Although these studies allowed direct comparisons between pre- and post-lesion responses of the same neurons, only a small number (a maximum of 4) neuron clusters could be recorded and their tuning properties bore no systematic relationship to one another.

In the present study, we documented both the peripheral and central effects of progressively enlarged SG lesions on 16 neuron clusters arrayed systematically across the ICC frequency gradient and recorded simultaneously. The progressively enlarged lesions produced progressively enlarged silent regions (or notches) within the receptive fields of the affected ICC neurons. These effects suggest topographically precise convergence of a series of narrow band inputs onto ICC neurons.

METHODS

Multichannel recording probes were inserted into the inferior colliculus of 7 normal hearing cats, and pre- and post-lesion recordings were made after multiple lesions. In 4 additional animals, pre- and post-lesion CAP and DPOAE audiograms were recorded after single lesions. All animals were maintained in a facility approved by American Association for Accreditation of Laboratory Animal Care. All procedures were approved by the UCSF Committee on Animal Research and were conducted in accordance with the guidelines provided by the PHS/NIH Guide for the Care and Use of Laboratory Animals.

Surgical preparation

Each animal was tranquilized with an intramuscular injection of ketamine HCl (25 mg/kg) and acepromazine (0.2 mg/kg). An intravenous catheter was inserted into the cephalic vein, and a surgical level of anesthesia was induced and maintained by infusion of sodium pentobarbital. A tracheal cannula was inserted via a tracheostomy. Body temperature was continuously monitored and maintained using a rectal thermal probe and a thermostatically controlled warm water re-circulating blanket. Blood oxygenation, respiratory rate and heart rate were continuously monitored using a pulse oximeter (Ohmeda). In addition, somatic reflexes (e.g. corneal reflex and forelimb withdrawal reflexes) were monitored to ensure that a surgical (areflexive) level of anesthesia was maintained. A urinary catheter was inserted into the urethra and the urine output collected and monitored. Lactated Ringer's solution was continuously infused throughout the experiments to maintain normal levels of hydration. Prophylactic injections of antibiotics (e.g., Cefazolin 22 mg/kg) were administered twice daily. In addition, prophylactic doses of dexamethazone (1 mg/kg/hr IV) and mannitol (1–2 mg/kg/day IV) were given to prevent cerebral edema. The head was immobilized and held in position using a bar attached to the calvarium with self-tapping screws and dental acrylic and mounted in a magnetic base. The external ear canals on both sides were opened near the bony annulus. The auditory bulla on the left side was surgically exposed and then opened to permit clear visualization of the round window.

Sound generation and delivery

An Intel based microcomputer was used to control the presentation of acoustic stimuli by signal generating hardware (Tucker-Davis Technologies, System II and System III). The effective

upper limit of this signal generation system was 40 kHz. Acoustic stimuli were presented through closed acoustic systems consisting of a Radio Shack supertweeter coupled via a metal casing to a plastic tube that was inserted and sealed into the external auditory canal. This system was calibrated with a B&K probe tube microphone (type 4182) and was calibrated during each experiment.

Compound Action Potential (CAP) audiograms

A silver ball 'active' electrode was placed in the round window niche of the left cochlea and fixed in place with cyanoacrylate glue. A silver wire 'reference' electrode was placed in the skin of the neck, and a silver wire ground electrode was inserted into the skin below the right ear. The voltage difference between the active and reference electrodes was amplified (World Precision Instruments DAM50 pre-amplifier and a Tektronix 5A22N plug-in amplifier) with band-pass settings of 100 Hz – 10 kHz and amplified 100,000x. The amplified output was displayed on an oscilloscope and digitized at 20 kHz and recorded for off-line analysis. The left cochlea was stimulated with 15 ms tone bursts having a 1 ms rise/fall time. Alternating tone-bursts were inverted in order to cancel the cochlear microphonic. Responses to 50–100 repetitions were averaged at each stimulus frequency and level. Frequencies were varied in steps of ¼ – ⅛ octave. Averaged responses from below threshold to 30 dB above threshold in 5 dB steps were obtained at each frequency. CAP thresholds were estimated using visual criteria applied to the averaged responses. CAP audiograms (plots of threshold vs. frequency) were constructed both immediately before and immediately after each SC lesion.

Distortion Product Otoacoustic Emission Audiograms (DP-grams)

Two primary tones were presented simultaneously to the left cochlea by two ER-2 insert earphones (Etymotic Research). The primary tone frequencies were maintained in a ratio of 1:1.2 with the lower primary at approximately +10dB re: the higher primary, while the lower primary was swept in ⅛ octave steps from 8 to 32 kHz. The acoustic signal in the external auditory meatus was recorded using an ER-10C (Etymotic Research) microphone, digitally sampled at 100 kS/s and analyzed off line using custom software written in Matlab.

ICC Recording

After exposure of the right IC, a 16-channel, single-shank silicon recording probe (NeuroNexus Technologies, Ann Arbor, MI, USA, (model a1x16-5mm 100 – 177 or –433) was inserted into the ICC. The silicon shank of this probe was 5 mm long, 15 μm thick, and a maximum of 240 μm in width, tapering to a sharp point at the tip. The probe had iridium-plated recording sites spaced linearly at 100 μm increments. Site impedances were typically 300 kOhms. The recording probes were mounted in a custom-built headstage that was held by a micromanipulator. Using the micromanipulator, the probes were inserted into the ICC along a standard trajectory that was in the coronal plane, passing from dorsolateral to ventromedial at an angle of 40° off the sagittal plane. This trajectory is approximately parallel to the ICC tonotopic axis with characteristic frequency (CF) increasing with depth. Penetration depth was adjusted using responses to acoustic tones until probe-site CFs spanned an appropriate range of frequencies, approximately 8 kHz to approximately 25 kHz, and the CFs were arrayed monotonically from low to high frequencies. This procedure effectively ensured that recordings were made from the central rather than the external nucleus.

To mechanically stabilize the recording probe, a 1% solution of warm liquid agarose was injected into the space below the parietal bone to cover the exposed nervous tissue. After agarose solidified, it and the parietal bone of the calvarium were covered with dental acrylic encasing the distal portion of the probe's printed circuit board. This sealed the opening in the skull and rigidly fixed the probe in place. Once the recording probe was fixed in place, the

animal was repositioned to allow access to the left cochlea, and the ear bar was reinserted and sealed into the left ear canal and the system was re-calibrated.

Multi-unit signals from recording probes were passed through a headstage, amplified using custom-built pre- and post-amplifiers, and bandpass filtered (700 – 3000 Hz). The amplified and filtered signals were digitized at 20 kHz using a multifunction board (model PCI6071E, National Instruments, Austin, TX). Experiment control, stimulus generation, data acquisition, data analysis and display were carried out using custom software written in LabView (National Instruments, Austin, TX, USA) and Matlab (The MathWorks, Natick, MA, USA). Spikes were identified in real time as events that crossed and re-crossed threshold amplitude within 0.4 ms as described previously (Snyder et al., 2007; Bonham and Litvak, 2008). In brief, event threshold amplitudes were determined independently for each recording site by measuring the RMS amplitude of a 1 s sample of spontaneous activity immediately prior to recording each response area, then multiplying that value by 3.5. This procedure allowed the threshold amplitudes to be adjusted for each recording site relative to the spontaneous activity recorded at that site. A standard multiplier value of 3.5 was chosen so that counted events were judged to arise from one to a small number of units depending upon the event sizes and their spontaneous rates (see Supplement Figure 1). CAP thresholds and FRAs at each ICC site were recorded before and after exposing the round window, opening the round window and each cochlear lesion.

Data collection and analysis

Events identified as spikes (see below and Supplement Figure 1), analogue waveforms, and spike times along with stimulus parameters were saved in a disk file for later analyses. Tones were presented in pseudo-randomized order over a range of frequencies and levels. Tone frequencies usually varied across ~4 octaves in 1/8 octave steps. The exact frequency limits varied among animals, depending upon the range of CF recorded, but these limits were held constant within an animal for an entire experiment. In no animal did we present tones below 2 kHz or above 40 kHz. Stimulus level usually varied over a range of 60–80 dB in steps of 5–10 dB. Frequency response areas (FRAs) were constructed by presenting each tone 4 times. The average number of spikes evoked by each tone was displayed in frequency vs. level in dB SPL (F/L) space. Responses were represented by vertical lines whose height was proportional to the magnitude of response (spontaneous activity was subtracted) elicited by each 50 ms tone plotted at the appropriate F/L coordinate, scaled so the maximum response evoked by any tone fit into the space allotted to a 5 dB level step (Figure 1). Characteristic frequency (CF) and threshold at CF were estimated from these line plots. Threshold was estimated as the lowest stimulus level to evoke a response consistently greater than spontaneous activity. CF was estimated as the frequency that evoked the largest response at the lowest threshold. If two or more adjacent frequencies elicited the same response amplitude at threshold, CF was estimated as the mean of those frequencies. Since response areas were constructed using 8 frequency steps per octave and level steps of 5 dB (or in a few cases 10 dB steps), CF was estimated to the nearest ± 1/16 octave, and threshold was estimated with a maximum accuracy of ± 5 dB. The pre- and post-lesion rates were normalized relative to maximum pre-lesion rates for each response area. Rate differences were computed by subtracting the normalized pre-lesion rate from the normalized post-lesion rate at each F/L combination. Once these rate differences were computed for each F/L combination, they were plotted as lines with positive values (post-rates > pre-rate) plotted in red and negative values (post-lesion rate < pre-lesion rate) plotted in black.

Sumner et al., 2008 categorized the lesion-induced receptive field changes into 4 types. As described by Sumner et al. (2008), Type 1 changes were those that showed simple excitatory losses at frequencies corresponding to the lesion frequencies. These excitatory losses could be

either above or below CF (Type 1a and1b, respectively), and sometimes produced notched FRAs. Type 2 changes showed simple off-CF gains in excitation occurring within the boundaries of the pre-lesion receptive field. These off-CF gains usually corresponded to the lesion center frequency (LCF), and occurred within the pre-lesion excitatory receptive field either above or below CF (Type 2a and 2b). Type 3 changes showed excitatory gains outside the pre-lesion receptive field (Type 3a and 3b). Type 4 changes showed both gains and losses of excitation either above or below CF (Type 4a and 4b) or both (Type 4c). These changes are particularly interesting because they produced shifts in CF and changes in IC frequency organization without a change in threshold. To Sumner et al.'s 4 types of lesion-induced changes (Figure 2), we added a fifth or Type 0 change, which describes neurons whose responses were unaffected by the lesions and no pre-lesion responses at lesion frequencies.

Spiral ganglion (SG) lesions

Acute SG lesions were created after exposing the round window, recording an initial CAP audiogram and recording at least one set of FRAs. Subsequently, the round window membrane was incised. A small amount of perilymph was aspirated to allow better visualization of Rosenthal's canal. All the lesions were made through an intact round window, i.e., without enlarging the perimeter of the round window, and in many cases with only a narrow slit in the round window membrane. This approach limited our choice of lesion locations to the high frequency region of the cochlea, the hook and the basal portion of the 1st cochlear turn. In 4 experiments lesions were made manually by curettage with a 34-gauge hypodermic needle. The bone overlying an approximate 1 mm segment of Rosenthal's canal was removed and the subjacent SG destroyed. These lesions have been described in our previous publications (Snyder et al., 2000; Snyder and Sinex, 2002). In the remaining 3 experiments, lesions were made using an Nd:YAG Minilase III-10 laser (New Wave Research, Inc.) equipped with a second harmonic generator and 2 dichroic mirrors to generate an output wavelength of 532 nm. The laser head was mounted on a motorized X-Y stage consisting of 2 orthogonally arranged digitally controlled stages (Newport, model 426). The 5mm beam diameter of the laser head was focused to a spot size of approximately 250 μm using a 200 mm quartz lens. The X-Y position of the beam was controlled visually by custom software (LabView™) running on a laboratory computer. The entire laser head, X-Y stage and lens system was mounted on a manual rack and pinion Z arm so that the beam could be focused on Rosenthal's canal (see Supplement Figure 2). At each location, Rosenthal's was irradiated with 10 pulses in 1 sec at an intensity of 1–2mJ/pulse. This level of irradiation produced a just discernible change in appearance of Rosenthal's canal from gray to white. After irradiation, the laser was moved to an adjacent and slightly overlapping location and the process was repeated (Fig. 3). Small manual or laser lesions (<0.5 mm in length) produced no or only very small changes in the CAP audiograms and produced no measurable changes in post-lesion response areas. Therefore, most lesions were progressively enlarged in increments of 0.5 – 1mm. When a lesion of the desired size was made, the perilymph was replenished with Ringer's solution, the round window was resealed using a disk of Saran Wrap™ to prevent further leakage of perilymph, and physiological recordings were made.

Although we always attempted to make lesions at cochlear frequencies that were sufficiently low that some of our recording sites had CFs above and some below LCF, most recording sites had CFs below the lesion frequency. This bias occurred because our lesions were made through the round window, i.e., restricted to high frequency locations, and our recording sites were arrayed along the tonotopic gradient from 2–25 kHz. Therefore, most of our recording sites had CFs below 20 kHz and most of our LCFs were between 16 and 25 kHz.

Histology

After the final recordings were made, some of the lesioned cochleas were perfused with fixative consisting of 2.5% paraformaldehyde and 1% glutaraldehyde in 0.1M phosphate buffer. After cochlear perfusion, the animal was given an intravenous overdose of Nembutal and perfused transcardially with lactated Ringer's solution containing 5% dextrose followed by the same fixative to which 5% sucrose was added. The cochleas were removed from the skull and allowed to sit in fixative @ 4°C overnight. They were then rinsed in 0.1M phosphate buffer and immersed in a solution of 1% osmium tetroxide in 0.1 M phosphate buffer for 24 hrs at 4° C. They were rinsed in phosphate buffer, dehydrated in ethanol and embedded in plastic. After embedding 2– 4 μm thick-sections were cut radially through the osseous spiral lamina at the level of the lesion to document the extent of the lesion.

RESULTS

In this study the response areas of neuron clusters were recorded in 7 animals using 16 channel silicon probes before and after up to 6 progressively enlarged spiral ganglion lesions. A broad range of lesion effects were observed in the matrix of more than 300 recorded response areas after these progressive lesions; effects were dependent upon LCF and range of the frequencies affected by the lesion, the CF the neurons and the animal. In order to describe these diverse effects, we shall first give an anatomical description of the lesions and their effects on cochlear physiology. We shall begin our description of the central lesion effects by presenting pre- and post-lesion frequency response areas of representative ICC neurons after small, medium and large sequential lesions in 2 animals. These response areas include each of the 5 categories of lesion-induced response changes. We will then illustrate the response changes induced by single large lesions across a series of neuron clusters with CFs distributed across the lesion frequencies in each of 3 animals. Finally, the results will be summarized by tabulating relative frequency of the lesion-induced changes observed in all neuron clusters recorded.

Anatomy of Spiral ganglion lesions

Initial small lesions were typically centered at approximately 2 mm from the basal end of the spiral ganglion at the junction of the hook and basal turn, a cochlear location where ganglion cells were tuned to frequencies between 16 and 24 kHz. Figure 3 shows an example of one such lesion. This lesion was produced by intentional over-exposure of the ganglion to laser irradiation. In addition, for purposes of this illustration, the round window membrane has been removed completely and all the perilymph has been aspirated. The lesion can be seen in the center of the round window immediately after laser irradiation. The osseous spiral lamina (OSL) and basilar membrane (white arrow) can be seen below the upper edge of the round window. The blood clot over Rosenthal's canal (white circle) marks the perimeter of the lesion. This abnormally high level exposure was used so that the lesion could be documented easily due to the extravasated blood, a feature normally absent from our laser lesions. The lower exposure levels that we normally used produced lesions that were difficult to document *in vivo*. Most initial lesions were made at the junction of the basal turn and the cochlear hook and then enlarged in both the apical and basal directions in 3–6 steps, each approximately 0.5 – 1 mm in length.

Figure 4A shows a histological radial section through the osseous spiral lamina of a normal animal. The organ of Corti lies to the right; the modiolus is toward the left. In this section intact spiral ganglion cells and their myelinated axons can be seen filling Rosenthal's canal. Figure 4B shows a similar section through a typical single laser lesion of Rosenthal's canal. Although there are a few remaining ganglion cells around the periphery of this lesion (arrows), most ganglion cell bodies and their myelinated axons are destroyed. In this and most experimental lesions there was little evidence of extravasated blood, most remote blood vessels (asterisks)

appeared intact and the osseous spiral lamina bordering the scala tympani, the region of the cochlea most directly illuminated by the laser, appeared intact throughout the length of the lesion.

Pre- and post-lesion CAP and DPOAE audiograms

We documented the physiological effects of SG lesions on cochlear function by constructing tone-evoked CAP audiograms before and after each lesion. When the lesions were enlarged to the maximum employed in these studies (3.5 – 4 mm), they produced significant elevations in CAP threshold over a frequency range of 1–1½ octaves centered at frequencies between 15–20 kHz. In Figure 5 pre-lesion CAP audiograms are plotted in magenta and post-lesion audiograms in red. The CAP difference audiogram (plotted in black) was computed by subtracting pre-lesion from post-lesion thresholds. In most cases, approximately 1 hr separated the pre- from the post-lesion threshold estimates, but these estimates and their differences were stable (within the resolution of our measurements) over the course of several hours. In the example shown in Figure 5, the CAP difference audiogram indicates a clear (>10dB) elevation in threshold beginning at about 13 kHz and reaching a maximum loss, ~30 dB, at about 25 kHz. Pre-lesion, post-lesion and difference DP-grams after the same lesion are illustrated in Fig. 5B. Despite some noise, there is less than a 5 dB change in the amplitude of the 2F1-F2 component across the range of primary frequencies encompassed by the lesion frequencies (15 – 32 kHz). In Figure 5C the mean CAP difference audiogram and mean difference DP-grams from this and a second animal that experienced a similar lesion are plotted. LCF in both animals was 25 kHz. Mean CAP thresholds (black) showed a loss in sensitivity beginning at 16 kHz and a peak loss of 35 dB at 25 kHz. In contrast, the mean 2F1-F2 amplitude changes were scattered around zero. Thus, we observed only small changes in distortion product (DP) amplitudes despite large increases in CAP threshold. If DP amplitudes are a measure of outer hair cell function, then these results are consistent with the notion that spiral ganglion lesions silenced restricted sectors of the auditory nerve array without altering organ of Corti or basilar membrane function.

Responses to sequentially enlarged lesions at single ICC sites

Tone-evoked CAP thresholds and difference audiograms after 3 sequentially enlarged SG-lesions in one animal (Figure 6) indicate that these lesions maintained a center frequency of approximately 29 kHz and that the threshold shifts and range of affected frequencies increased as lesion size increased. In this experiment the range of affected frequencies reached a maximum of ~1 octave and the maximum threshold increase was ~40 dB.

Examination of post-lesion and difference FRAs shows that opening of the round window had little effect on the receptive fields of ICC neurons. Usually they showed no change in threshold or CF (Fig. 7B&F). Occasionally, there were small randomly distributed losses (black) or frequency specific gains (red) in excitation (Fig. 9B&G) observed after opening the round window. In contrast, even small lesions, which produced only small changes in the CAP audiogram, produced clear shifts in threshold among ICC neurons with CFs at LCF (Fig 7G). Among these neurons there was an increase in threshold at the tip of the pre-lesion area, but little change in response amplitude at higher levels (Figs. 7C, G). As the size of the lesion was increased, the losses of excitation occurred at higher levels and across a wider range of frequencies. The losses were greatest at the LCFs, which in Figure 7 corresponded to these neurons' pre-lesion best frequency or BF, the frequency that produced the largest response at a given stimulus level. No or only modest changes were observed at other frequencies (Figs. 7G & H). The changes observed in these responses are representative of the simplest lesions-induced changes and we have categorized them as Type 1 changes. They show losses of excitation (black difference responses) within the pre-lesion excitatory response area with minimal gains or unmasking from inhibition of excitation (red difference responses).

More complex post-lesion changes in ICC responses were observed in other animals despite similar changes in the CAP audiogram. For example, the pre-, post- and difference audiograms in Fig. 8A illustrate tone-evoked thresholds before and after the largest of 6 lesions. This lesion produced a maximum threshold shift of 45 dB centered at ~17 kHz and produced threshold changes extending across 1.6 octaves from 10 to 30 kHz. The threshold shifts after this and 2 smaller lesions demonstrate that there were progressive increases in threshold from ~20 dB to ~45 dB and shifts in the peak-loss frequencies from ~21 kHz to ~17 kHz (Fig. 8B). The shift in frequency of the peak-loss undoubtedly occurred as a result of an asymmetrical enlargement of the lesion toward the cochlear apex. Below 10 kHz there were only small ($\leq \pm 15$ dB) changes in CAP thresholds after all 6 lesions.

The next three figures describe the lesion-induced changes in ICC response areas before and after the lesions shown in Figure 8. These are more complex than those seen in Figure 7 in that they show both lesion-induced gains as well as losses of excitation and these gains/losses are seen to be dependent upon the neurons' locations, i.e., with BFs below (Fig 19), equal to (Fig. 10) or above LCF (Fig. 11). The lesion-induced changes at these sites illustrate not only lesion induced losses but also lesion-induced gains in excitation.

In Figure 9 the neurons recorded at site 9, 800 μm from the most superficial site, were tuned to frequencies below the lesion frequencies. When the cochlea was intact, these neurons had a minimum threshold of 40 dB SPL and a CF near 14 kHz (Fig. 9A). After the opening of the round window but before any lesion, the sensitivity of these neurons increased slightly, approximately 5 dB, although CF itself was unchanged. This is consistent with a 5–10 dB *decrease* in CAP threshold for frequencies between 5 and 25 kHz (blue curve in Fig. 9B, F). As a consequence of this broad sensitivity increase, the excitatory response amplitudes at many F/L combinations increased slightly after opening the round window, and response differences (Fig. 9F) show net gains in amplitude (red lines) across most of the excitatory region. This post-round-window-opening effect was seen at all sites in this experiment.

After a small lesion (blue curve, Fig. 9C, G), there was a 20 dB loss in CAP sensitivity centered at 21 kHz and a small (5dB) elevation in CF threshold at this site to 35 dB SPL relative to the responses recorded after the round window was opened. If this decrease in sensitivity had occurred throughout the excitatory area at this site, decreases in response amplitude would have been expected throughout its excitatory region. However, as the black response lines in Figure 9G indicate, there were excitatory losses across 2 separate frequency regions: 1) at the lowest stimulus levels near CF and along the high frequency edge of the response area, and 2) in the low frequency tail. The CF losses after this small lesion occurred over a narrow range of levels and produced no change in CF at this site. The losses along the high frequency edge of the excitatory response area corresponded to LCF. The losses in the low frequency "tail" were far below the lesion frequencies as defined by the CAP audiogram. Such low frequency losses occurred in many response areas in this and other animals. In addition to the response losses, there were small excitatory gains (red responses, Fig. 9F) at frequencies near BF at a broad range of stimulus levels. This is a clear example of a Type 4 post-lesion change.

After the lesion was increased to a moderate size (Fig. 9D & H), CAP thresholds at frequencies near 20 kHz were increased by 30 dB (blue line). Neuron thresholds at CF (~15 kHz) were increased by an additional 5 dB to 45 dB (Fig. 9D), but the CF itself was unchanged. As can be seen in Fig 9H, there were additional losses of excitation at the tip, along the high frequency edge, and in the low frequency tail of the response area.

After the largest lesion (Fig. 9E & I), CAP thresholds at frequencies increased across a broader range of frequencies (from 30 to 10 kHz) and the threshold shift at LCFs (17–19 kHz) increased to 45 dB above pre-lesion levels. Consistent with this increased loss in peripheral sensitivity,

neuronal response losses surrounding CF spread further in frequency and occurred across a wider range of stimulus levels (~30 dB above threshold). Meanwhile, losses along the high frequency edge of the response area increased in magnitude and spread to lower frequencies (Fig. 9 I). These losses produced a distinct shift in CF of neurons at this location from 13.5 kHz to ~10 kHz, but only a modest shift in threshold, ~10 dB above that seen after opening the round window. Between the high and low frequency losses, there was a region of no loss or small excitatory gain (Fig. 9 I, red bars), a Type 1 change but with an additional loss of excitation in the low frequency tail.

Many of the same lesion-induced changes are seen at site #11, 200 μm deeper in the IC. Although the CF of neurons this site was only slightly higher than that at the previous site, the BF was significantly higher at approximately 21 kHz (Fig. 10A). After opening the round window, there was a broadly distributed increase in excitation among neurons at this site, but there was no change in their CF or BF (Fig. 10B, F), which is consistent with the results described Fig. 9 at this experimental stage. As seen in Figure 9, after progressively larger lesions, there were progressively larger excitatory losses (black responses, Figs. 10G, H & I) among these neurons. These losses occurred primarily in the low frequency tail and at LCFs along the high frequency edge of the response area. The magnitude and frequency distribution of these high frequency losses increased with successively larger lesion.

The high frequency losses in the responses of these neurons might be expected, since the BF of this site matched LCF, the frequencies at which the greatest losses in sensitivity occurred. However as seen at site #9, there were often also clear excitatory losses in the low frequency tails of the responses. In contrast with the high frequency losses, the low frequency losses shifted little in frequency or level as the lesion size was increased, but their magnitudes increased progressively. Like the high frequency losses at LCFs, the low frequency losses occurred even after relatively small lesions (Fig. 10C&G) and their growth in magnitude with lesion size eventually abolished most or all excitation at many F/L combinations (compare Figs. 10B with Fig. 10E).

In addition to the excitatory losses just described, there were clear excitatory gains observed near CF at high stimulus levels (red responses in Figs. 10 G, H & I). These gains are consistent with losses of inhibitory drive which is off-set from LCF. Regions of excitatory gain often increased non-monotonically with lesion size. As In this example, gains in excitation increased after lesions 2, 3 (not shown), 4 and 5 (not shown) and then decreased after lesion 6 (Fig. 10I). The increase and subsequent decline in excitatory gains occurred presumably because, as the lesion frequencies spread across the response area, they began to include the most potent excitatory and inhibitory frequencies, those at or near BF. It is interesting to note that the regions of excitatory gains were often separated from the regions of high frequency losses by a narrow region where there was little or no change in excitation (green arrowheads, Fig. 10G, H & I).

These excitatory gains at mid-frequencies and excitatory losses at high frequencies produced a distinct notch in the post-lesion response areas, in this case above CF, corresponding to LCF (green asterisks, Figs. 10C, D & E). When the lesion was enlarged the excitation losses increased in magnitude and spread to adjacent frequencies and levels. However, the excitatory gain also increased magnitude. Thus the notch in the response area became progressively more prominent, so that after the 5^{th} (not shown) and 6^{th} lesions (Fig. 10E & I) the response area had a “W” shape producing two CFs: one near 12 kHz and another near 24 kHz, with equal thresholds of 55 dB SPL, a Type 4 change. These dual CFs represent a significant change in the frequency organization of the IC, although their thresholds are significantly higher (~15 dB) than the pre-lesion threshold.

At sites with CFs above LCF in this experiment (Figure 11), two types of receptive field changes were conspicuous: a loss in excitation producing a notch in the response region below CF which corresponded to LCF and gains in excitation at frequencies both above and below it. The neurons at site #13 (Fig. 11) had a pre-lesion CF of near 27 kHz and an equally high BF of 25 kHz. Both CF and BF were above LCF (21–17 kHz depending upon lesion size). Thus the lesion occurred in the low frequency responses of these neurons. The most easily seen post-lesion change in these high frequency neurons was the loss of excitation at tone frequencies corresponding to LCF. In addition, however, there were gains in excitation at frequencies both above and below the lesion frequencies (Figs. 11G, H and I). The combination of losses of excitation at LCF and gains in excitation both above and below LCF produced a conspicuous notch (asterisks) in the response area (Figs. 11C, D & E). In addition, gains in excitation produced an FRA with two CFs: one near the original CF of 27 kHz and another at a much lower frequency (near 14 kHz). Although not demonstrated in Figure 11, excitatory gains at frequencies above LCF often also produced CF shifts in these high-CF neurons to even higher frequencies (see Fig. 14, sites #13 and #14). The post-lesion responses observed in Figure 11D & E represent Type 2 changes, i.e., the addition of evoked activity within the low frequency boundary of the pre-lesion response area without a clear CF shift. Alternatively, the "W" shaped response area in Figure 11C would be categorized as a Type 4 change. Thus there is a clear relationship between post-lesion response type and lesion size.

Effects of a single large lesion at several sequential sites with increasing CFs

The description of our results so far has been restricted to the effects of sequentially enlarged lesions at single recording sites. One of the conclusions that can be drawn from those data is that the lesion effects are systematically related to the size of the lesion. We will now consider the effects of single lesions on sequentially located sites with sequentially increasing CFs. Figure 12A shows pre-lesion FRAs recorded at 6 (of 12) even numbered probe sites affected by one lesion (shown in Figure 8A). The CFs at these sites increased progressively from 9.2 kHz (site #4) to 29 kHz (site #14). The post-lesion responses (middle row, Fig. 12B) and response differences (bottom row, Fig. 12C) reveal that a number of the lesion effects are systematically dependent upon the relationship between neuron CF and LCF.

As one scans from left to right across the post-lesion responses (Fig. 12 B), the pre-lesion response threshold tuning curves (black curve) pass over the CAP difference curve (blue curve). This progression illustrates that the losses in the post-lesion responses (red bars) are systematically related to the lesion frequencies. Relatively low frequency neurons (e.g., site #4, far left), had pre-lesion tuning curves that overlapped only slightly with the CAP difference audiogram. In these neurons there is little effect of the lesion on the post-lesion responses (Type 0 change). As the CF of the neurons shifted to higher frequencies (sites #6 & #8), the tuning curves began to overlap with the peak in the CAP difference audiogram, and there were progressively larger losses in excitation along the high frequency edge of the post-lesion responses (Type 1 changes). As CF continued to increase (sites #8 – #12), a notch appeared in the receptive fields at LCF accompanied by excitatory losses in the low frequency tails of the responses and some excitatory gains at frequencies just below LCF.(Type 4 changes). At locations with the highest CFs (site #14), the responses at frequencies above LCF are only weakly affected or enhanced and the responses below CF and at BF are greatly diminished or abolished (Type 1b changes).

Scanning the difference responses (Fig. 12C) from left to right in, one can see that initially there were losses primarily at the tips of the responses near CF. Then at higher CF sites, there were additional losses in the low frequency tails. At progressively higher CF sites, as threshold tuning curve edges began to overlap with LCF, losses occurred at the tips, tails and along the high frequency edges of the response areas (sites #8 & #10). At approximately site 12, the

response area BF became coincident with LCF and responses around BF were strongly reduced and response gains appeared both above and below BF (Type 4 changes).

Figure 13 shows another example of the progression of lesion effects across 6 contiguous sites. At these sites, the effects on neurons tuned to the lowest frequencies (site 9) showed losses at the tip frequencies and modest losses at low frequency (Type 1b). The lesion-induced changes in responses of neurons tuned to higher CFs (sites 10–14) show progressively greater losses along the high frequency edges of their receptive fields, notches in their receptive fields and progressive gains in excitation at frequencies higher than their original receptive fields (Type 4 changes). In some cases, when LCF coincided with the pre-lesion CF (sites 13 & 14), the losses at CF and the gains in excitation above CF produced responses with higher frequency CFs than the pre-lesion responses (Type 4b change).

The response areas shown in Figure 14, display a somewhat different pattern of response change as a function of CF than that seen in the previous two experiments. Neurons tuned to lower CFs (sites #6 & #8) displayed post-lesion increases in excitation along their low frequency edges rather than low frequency losses. In some cases (e.g., site #6), this additional excitation produces a second, lower frequency peak in the receptive field and a notch in the receptive field. Although this notch looks superficially like the notches seen previously in Type 4 changes, it is clearly different. It arises solely as a consequence of a frequency specific gain in excitation which occurs beyond the low frequency boundary of the pre-lesion excitatory area in neurons tuned to frequencies well below LCF, a Type 3 change. Such low frequency gains in sensitivity have been reported following acoustic trauma for single neurons in both the IC and DCN (Wang et al., 1996; Salvi et al., 1996). Neurons recorded at deeper, higher CF sites in this experiment show simple losses in excitation (Type I changes) within the boundary of the pre-lesion receptive field similar to that observed in Figure 7.

Summary—Table I summarizes the relative frequency of occurrence of the 5 types of lesion-induced response changes observed in these experiments after the largest lesion in each experiment. The most frequently occurring change was Type 0; 36% of ICC sites showed no change or small global gains or losses (DC shifts) in their post-lesion response amplitudes with no change in their CFs or in their minimum thresholds. Type 0 changes occurred exclusively in neurons tuned to frequencies remote from the lesion frequencies, and thus, their relative frequency of occurrence was strongly influenced by size of the lesion and range of neuronal CFs sampled by our recording probes. In our experiments even the largest lesions produced little or no change in CAP thresholds below 10 kHz, yet ~1/3 of our recording sites had CFs below this frequency. If our neuronal sample had been restricted to neurons with CFs *above* 10 kHz, virtually all would have shown some lesion-induced change in their receptive field.

Type 1 changes, a simple loss of excitation along the high or low frequency edge of the response producing residual post-lesion responses, were the most frequently observed post-lesion changes; neurons at 43% of recording sites, which showed a change, showed lesion-induced residual responses. This type of change resulted in a “passive” shift in CF with a small (usually less than 15 dB) shift in threshold. In contrast, the remaining 57% of lesion induced changes could not be explained by passive losses of excitation. Type 2 and Type 3 changes showed *increases* in excitation within (Type 2) or outside of (Type 3) their pre-lesion receptive fields without any excitatory losses or changes in CF. These changes were observed relatively infrequently (14% and 9% respectively), but they are among the most interesting for two reasons: First, since they appear without any observed losses in excitation, they must result from lesion-induced unmasking (or release from inhibition). Second, they occurred at sites with CFs remote from lesion-frequencies and at frequencies that were remote from the CF or BF of the pre-lesion response, i.e., at the edges of the excitatory response.

Type 4 post-lesion responses occurred at 34% of our recording sites that showed a post-lesion change in response. Type 4 response resulted from complex combinations of lesion-induced excitatory losses, which were often coupled with excitatory gains. The gains in excitation occurred across one frequency range whereas the losses occurred across another. This combination often produced dramatic shifts in CF and clear notches in the excitatory regions of these post-lesion response areas. The notches usually corresponded to the LCF and could be centered at frequencies above, at or below CF or BF. Type 4 responses would probably have been observed more frequently if our lesions had been larger or if our recording sites had been less widely distributed, that is, if more of our recording sites had been tuned to the lesion frequencies.

Along with the lesion induced excitatory losses of in the low-frequency "tails" of some neurons, the remote gains in excitation (Type 2, 3 and 4 responses) indicate remote frequency-specific interactions between direct and indirect afferents to the IC at frequencies distant from CF and distant from the lesion frequencies. These interactions are independent of the interactions between a neuron's CF or BF and the LCF.

DISCUSSION

Interaction between LCF and CF

Looking at the range and distribution of the types of post-lesion changes in the IC, it is clear that the type of change observed at any given recording site is dependent at least in part upon the relationship between its CF and the LCF. Neurons recorded at sites with CFs far from the LCF showed either no change or small, frequency independent shifts in their response amplitudes and/or threshold (Type 0 changes). Neurons at sites with CFs near but not at the LCF tended to show losses at CF and along their high or low frequency edges depending upon whether their CF was above or below the LCF (Type 1 changes). Neurons at sites with CFs at or very near LCF showed response losses in the center of their receptive fields at and around CF and/or at BF. These losses usually, but not always (Fig. 14B), produced notches in the excitatory response regions of these neurons corresponding to LCF and were often accompanied by (Figs. 10 & 11) excitatory gains at other remote frequencies (Type 4 changes).

Finally, after some lesions, the dominant post-lesion change at sites with CFs *far below* LCF was a frequency specific gain in excitation, a Type 3 response (Fig 14, site 6). In these experiments, the excitatory gains were usually below the low frequency edge of the excitatory response areas of these low frequency neurons, i.e., below the side furthest from LCF. It should be remembered, however, that our lesion frequencies were restricted to relatively high frequencies (>15 kHz). It was, therefore, impossible for us to record from neurons with CFs sufficiently high and sufficiently remote from these high frequencies lesions for Type 3 changes to be observed on their high frequency sides. Interactions between LCF and CF are summarized in Figure 15.

Excitatory losses at lesion frequencies—In these experiments post-lesion excitatory losses at the "tips" of response areas were observed in all 7 experiments. The magnitude and frequency range of these tip losses varied and the greatest losses occurred at frequencies that corresponded to those regions where there was the greatest overlap between pre-lesion tuning curves and CAP threshold shifts. The tip losses increased in magnitude and the frequency range of the losses increased as the lesions were enlarged (e.g., Fig. 7). Response losses other than those near CF or at lesion frequencies were also observed in some animals, but only when near CF losses were also observed. For example, the low frequency (tail) losses seen in Figure 12 were observed in two experiments at all recording sites where there were both low-frequency tails and high frequency losses.

The largest excitatory losses usually occurred at or near LCF regardless of the frequencies to which the neurons were tuned (Figure 15 A – F). Therefore, neurons tuned to frequencies below the LCF showed excitatory losses only along their high frequency edges (Fig. 15A–B); those tuned to frequencies at or near LCF showed the greatest excitatory losses at or near CF and BF and frequently showed notches in their post-lesion response areas (Fig. 15C–E); neurons tuned to frequencies above LCF showed losses and notches along their low frequency edges below CF and BF (Fig. 15F). Thus post-lesion CFs (yellow arrows) often remained constant (Fig. 15A–D) producing large post-lesion inflections in the post-lesion CF gradient until a critical tipping point (between D & E in Figure 15) is reached. At this point CF shifts dramatically from below LCF to above it, while above this point CFs follow the normal pre-lesion sequence generating a discontinuity in the CF gradient. In addition, post-lesion ICC threshold changes are relatively modest, and silent regions in the ICC have never been observed in our experiments. Thus even neurons, which showed only simple excitatory losses without concomitant excitatory gains, displayed clear shifts in CF.

Although these Type 1 responses displayed clear elevations in threshold, these shifts were relatively modest. Depending upon their tuning curve widths and the range of the lesion frequencies, ICC post-lesion Type 1 thresholds were typically only 20–30 dB higher than pre-lesion thresholds, but could be 40 dB or more. These simple losses in excitation have been characterized by some as “passive” or “pseudoplastic” changes (Kaltenbach et al., 1992) and the responses called “residual” responses (Robertson and Irvine, 1989; Rajan et al., 1993) suggesting that they are similar to those observed in auditory nerve fibers following acute and chronic acoustic trauma (Kiang et al., 1976; Liberman and Kiang, 1978; Liberman and Mulroy, 1982; Robertson, 1982).

However, the CF and threshold changes observed in auditory nerve fibers after acoustic trauma (illustrated diagrammatically in Figure 15) differ significantly from even the simplest Type 1 post-lesion responses seen in ICC neurons after SG lesions. Among auditory nerve fibers tuned to frequencies higher than the lesion frequencies (Fig. 15A′ to F′), post-lesion CFs match the pre-lesion CFs (Kiang et al., 1976; Liberman and Kiang, 1978; Liberman and Mulroy, 1982), but post-lesion sensitivity losses at “tip” frequencies can be dramatic, commonly greater than 60 dB. In some cases the losses exceed the output of the stimulus system producing silent regions in the nerve (Robertson, 1982; Liberman and Dodds, 1984). Such silent regions have not been observed among ICC neurons except among very narrowly tuned neurons after large acoustic lesions spanning more than an octave (Fig. 7E). Concurrent with tip sensitivity losses, threshold *decreases* in ANF responses at low or “tail” frequencies (Fig. 15A′, C′, D′) can occur after acoustic trauma and can produce notches in ANF responses and “W”-shaped tuning curves (Fig. 15 C′ & D′). These “W”-shaped curves look superficially like the “W”-shaped response areas in the ICC, but they are clearly different. The notches in ANF responses after acoustic trauma are centered at frequencies below the lesion frequencies, and they are rarely more than 10 dB deep, whereas the notches in the ICC neurons are always centered at LCF. In addition, the pre-lesion to post-lesion elevations in threshold among ICC neurons can be more than 60 dB. Finally, after our mechanical and laser lesions, the thresholds of the affected auditory nerve fibers are infinite, whereas the thresholds of neighboring un-lesioned fibers are unaffected. For these reasons, even the Type 1 response changes observed in ICC cannot be considered “passive” in the sense that they simply reflect changes in the auditory periphery; a point made clearly by Norena and Eggermont (2003) for the response changes in cortical neurons after acoustic trauma.

In contrast to auditory never fibers, post-lesion CF shifts in ICC neurons are relatively large with concomitant relatively small threshold shifts. In addition, some ICC neurons show post-lesion threshold increases and response amplitude decreases at low tail-frequencies not observed in auditory nerve fibers (Figs. 10, 12 & 13). Although tuning curves in auditory nerve

fibers often have notches between their “tips” and “tails” after acoustic trauma similar to the notches seen in ICC after SG-lesions, the frequency locations of auditory nerve notches are unrelated to LCF, whereas the notches in ICC FRAs after SG-lesions are centered at LCF. These differences, which are summarized diagrammatically in Figure 15, have also been observed in models of post-lesion responses in central auditory neurons (Scholes et al., 2006;Sumner et al., 2008; Sinex unpublished observations).

It should be noted, however, that decreases in tail frequency thresholds producing notches between tip and tail responses have been observed in 80% (12/15) of “level tolerant” or I-type IC neurons recorded before and after acoustic trauma with above CF tones (Wang et al., 1996). But all neurons (22 of 22) with “open-V” tuning curves showed no or little change in their responses, and all tuning curves they recorded after acoustic trauma (40 of 40) showed *almost no change in CF or CF threshold*. Thus, although the changes in responses of some IC neurons after acoustic trauma resembled those observed in auditory nerve fibers, nevertheless the trauma induced changes in the two auditory areas differ significantly.

Post-lesion gains in excitation or losses of inhibition—Gains in excitation were observed both inside and outside the bounds of pre-lesion receptive fields and these gains could occur either above or below the pre-lesion CF. If excitatory gains occurred outside the pre-lesion FRA, they usually occurred on the high or low frequency side of CF but not both. If they occurred at low enough stimulus levels, the resulting “W” shaped response areas (called Type 4 responses) could produce shifts in CF of up to an octave with no change or even a decrease in minimum threshold. If they occurred inside the boundary of the pre-lesion FRA, they could change a neuron’s BF without changing its CF or minimum threshold (a Type 2 response).

One mechanism for these excitatory gains is unmasking from inhibition, i.e., the release of excitation from evoked or spontaneous inhibition. This inhibition is presumed to suppress excitatory activity that becomes observable only when the inhibition is withdrawn by the lesion. Such lesion-induced unmasking has been reported in auditory, visual and somatosensory cortices (see, Calford, 2002 for review) but it has been reported only rarely in subcortical areas (Irvine and Rajan, 1998; Irvine et al., 2003). Post-lesion responses displaying unmasking (Types 2, 3 & 4) together account for 57% of the lesion-induced changes observed in ICC neurons. Type 2 & 3 changes, i.e., excitation increases inside (Type 2) and outside (Type 3) the pre-lesion response area without concomitant excitatory losses or changes in CF, occurred in 23% of response areas which showed a post-lesion change. It is worth noting that these percentages approximate the proportion of lesion induced receptive field changes observed by Sumner et al. (2008) in their “basic multi-compartmental” computational model of ICC neuron receptive fields.

Remote excitatory losses—Additional excitatory losses were often observed at frequencies far from LCF and far from BF. These remote losses occurred across broader frequency ranges than those at or near BF. The two sets of losses, when they occurred, were usually separated by a region of activity that was either unaffected by the lesion (Figure 12, site 10) or a region of excitatory gains (see Figure 10). This observation alone does not distinguish between two complementary models: 1) low-frequency responses evoked by activity in AN fibers with the same BF as the IC neuron, and 2) low-frequency responses evoked by activity in low-BF fibers. In either case responses evoked at intermediate frequencies must originate in or be modulated by activity originating in AN fibers with different BF(s). Otherwise, the pre- to post-lesion difference FRA would exhibit a loss of excitation at intermediate frequencies similar to the losses observed at BF and at low frequencies.

Mechanisms for post-lesion effects—At the moment we can only speculate regarding the mechanisms for the reported SG-lesion effects. However, one model accounts for much of

the pre- and post-lesion behavior observed in ICC neurons (Scholes et al, 2006; Sumner et al., 2008). This model hypothesizes several features of ICC afferent inputs among which are: 1) that each ICC neuron receives spectrally convergent excitatory and inhibitory inputs each representing a narrow range of BFs, 2) that the dendritic locations of these inputs are aligned and tonotopically organized such that only excitatory afferents tuned to the ICC neuron's BF terminate on its cell body and those tuned to successively more remote frequency bands terminate on its successively more distal dendritic segments, and 3) that the dendritic locations of inhibitory inputs from each band are systematically displaced distal to its excitatory inputs. Given these features, removal of excitatory inputs from a restricted BF range will produce a corresponding notch in the neuron's FRA and removal of inhibitory influences on adjacent frequency-band afferents will reveal (unmask) their excitatory inputs. It is beyond the scope of this paper to elaborate on all the predictions and limitations of this model. Suffice it to say that, although their model reproduces many of the observed pre- and post-lesion responses of ICC neurons, other models could result in similar processing (Sinex, unpublished observations).

Time course of changes produced by SG lesions

SG-lesions produced narrow-band elevations in post-lesion CAP thresholds without affecting without affecting cochlear signal processing. This is a major difference between this and other lesion methods (Kiang et al., 1976; Liberman and Kiang, 1978; Robertson, 1982; Liberman and Mulroy, 1982; Calford et al., 1993; Salvi et al., 1996; Wang et al., 1996, Kiang et al., 1976; Liberman and Mulroy, 1982; Harrison et al., 1991, 1993, 1995, 1996; Salvi et al., 1982, Robertson and Irvine, 1989; Rajan et al., 1993; Irvine et al., 2000, 2003) which produce idiosyncratic changes in cochlear signal processing that may take weeks or even months to stabilize. The changes observed following SG lesions were complete as soon after the lesion as they could be measured. They were stable. They were observed to remain stable for periods of many hours to a few days after the lesion (Snyder and Sinex, 2002) and continuous high level stimulation with acoustic tones or noise bands had no effect on them (unpublished observations). In this respect SG-lesion induced changes observed in the ICC are comparable to the changes observed in somatosensory cortex after somatic peripheral nerve lesions or digit amputations (Calford and Tweedale, 1988; 1991a, 1991b; Kolarik et al., 1994).

Both these lesion-induced changes in the auditory and somatosensory systems differ from those observed in visual cortex after retinal lesions. Retinal laser lesions produce immediate changes in cortical retinotopy, but the changes are progressive changing over the course of 1–2 hours after the lesion (Schmid et al., 1995; Calford et al., 1999). These progressive changes, however, have been attributed to changes in the recovery of the retinas from non-specific trauma in the lesioned eye (Calford et al., 1999). We observed no such post-lesion recovery in the cochlea after our SG lesions.

The current results demonstrate that acute changes in the ICC are composites of both immediate losses of excitation and gains in excitation. The gains are presumed to occur as a result of withdrawal of inhibition (see Figs. 11C & 12C). We have observed no significant post-lesion modulation of ICC responses changes. We routinely recorded ICC responses at all 16 probe sites after several post-lesion intervals up to 12 hrs without observing any additional changes aside from those that were immediately observable. This is also true for post-SG-lesion changes observed in auditory cortex (Snyder and Sinex, 1998). Moreover, these changes occur without any special conditioning. They do not require any particular post-lesion stimuli to evoke them nor are they modified by post-lesion stimulation. The relatively rapid time course of these changes and their post-lesion stability are worth noting, since they preclude several mechanisms of plasticity, such as anatomical sprouting and synaptic plasticity resulting from

long term potentiation or long term depression, which might be invoked to explain post-lesion changes.

Tonotopic significance of lesion-induced changes

ICC receives tonotopically organized afferents from a variety of auditory brainstem nuclei that project into the IC as flattened sheets or laminae. Since 75% of ICC neurons have flat or disc-shaped dendritic fields that run parallel to these afferent sheets, it is not surprising that most electrophysiological studies report that ICC neurons have narrowly tuned "V" shaped response areas and would not be expected to receive spectrally convergent input (see Oliver, 2005 for review). Despite this strong evidence, other studies have provided convincing evidence for spectral convergence across broad frequency bands onto ICC cells. This evidence is derived from measurements of the interactions between diverse spectral components in spectrally complex stimuli (Krishna and Semple, 2000; Biebel and Langner 2002; Li et al., 2006; Portfors and Wenstrup, 2002; Nataraj and Wenstrup, 2005, 2006; Sinex et al., 2002; Sinex 2005; Sinex and Li, 2007) and from measurements of excitatory and inhibitory receptive fields (Rose et al., 1963; Ryan and Miller, 1978; Willot et al., 1984; Semple and Kitzes, 1985); Rees and Palmer, 1988; LeBeau et al., 2001; Yang et al., 1992; Ramachandran et al.,1999; Xie et al., 2006). An example of broad-band spectral interactions is illustrated by Li et al. (2006), who stimulated IC neurons in the anesthetized chinchilla with SAM tones whose carrier frequencies were outside the neuron's response area. Nevertheless, these SAM tones modulated the neuron's responses to sustained CF tones despite the fact that neither the SAM tones nor any of their components evoked activity when presented alone. An example of broad-band receptive fields is illustrated by Li et al. (2006), who used whole cell recordings in the ICC to explore the frequency distribution of spikes and excitatory and inhibitory post-synaptic potentials. They found that tones evoked complex post-synaptic potentials over a frequency range that was twice as wide as their receptive fields as defined spike discharges.

The results in this study are in agreement with the studies indicating spectral convergence onto ICC neurons cited above. Further, they suggest that frequency responses of ICC neurons are composites or mosaics of discrete convergent frequency channels topographically arrayed along their receptive surfaces. Each channel evokes activity across a narrow range of frequencies and the activity from each channel is ultimately traceable to a specific, restricted sector of the spiral ganglion. Elimination of the input from a channel produces notched losses at the corresponding frequencies within the excitatory response areas of ICC neurons. The results suggests that excitation evoked by 18 – 20 kHz tones in all IC neurons, for example, is dependent upon and ultimately derived from auditory nerve fibers tuned to 18 – 20 kHz. Destruction of these cells removes the excitation evoked across that frequency range, but leaves intact the excitation evoked by fibers tuned to adjacent frequencies (e.g., 16–18 kHz & 20–22 kHz) or may release excitation at these adjacent frequencies or frequencies remote from them.

Supplementary Material

Refer to Web version on PubMed Central for supplementary material.

Acknowledgements

The authors would like to thank Drs. CJ Sumner, JH LaVail and an anonymous reviewer for their thoughtful reading of and comments on this manuscript. We would also like to acknowledge support by NIDCD grants DC03549 and DC00341

ABREVIATIONS

AN

Auditory nerve

BF
Best frequency

CAP
Compound action potential

CF
Characteristic frequency

CNS
Central nervous system

DP
Distortion product

DPOAE
Distortion product otoacoustic emission

F/L
Frequency & level

FRA
Frequency response area

IC
Inferior colliculus

ICC
Central nucleus of the inferior colliculus

LCF
Lesion center frequency

Nd:YAG
Neodymium-doped yttrium aluminium garnet

OSL
Osseous spiral lamina

SG
Spiral ganglion

LITERATURE CITED

Biebel UW, Langner G. Evidence for interactions across frequency channels in the inferior colliculus of awake chinchilla. Hear Res 2002;169(1–2):151–68. [PubMed: 12121748]

Brown M, Webster WR, Martin RL. Intensity and frequency functions of [14C]2-deoxyglucose labeling in the central nucleus of the inferior colliculus in the cat. Hear Res 1997a;104(1–2):73–89. [PubMed: 9119768]

Brown M, Webster WR, Martin RL. The three-dimensional frequency organization of the inferior colliculus of the cat: a 2-deoxyglucose study. Hear Res 1997b;104(1–2):57–72. [PubMed: 9119767]

Brunso-Bechtold JK, Thompson GC, Masterton RB. HRP study of the organization of auditory afferents ascending to central nucleus of inferior colliculus in cat. J Comp Neurol 1981;197:705–722. [PubMed: 7229134]

Calford MB, Tweedale R. Immediate and chronic changes in responses of somatosensory cortex in adult flying-fox after digit amputation. Naure 1988;332:446–448.

Calford MB, Tweedale R. Acute changes in cutaneous receptive fields in primary somatosensory cortex after digit denervation in adult flying-fox. J Neurophysiol 1991a;65:178–187. [PubMed: 2016636]

Calford MB, Tweedale R. Immediate expansion of receptive fields of neurons in area 3b of macaque monkeys after digit denervation. Somatosens Mot Res 1991b;8:249–60. [PubMed: 1767621]

Calford MB, Schmid LM, Rosa MG. Monocular focal retinal lesions induce short-term topographic plasticity in adult cat visual cortex. Proc Roy Soc B: Biological Sciences 1999;266:499–507.

Calford MB, Rajan R, Irvine DR. Rapid changes in the frequency tuning of neurons in cat auditory cortex resulting from pure-tone-induced temporary threshold shift. Neuroscience 1993;55:953–64. [PubMed: 8232905]

Calford MB. Dynamic representational plasticity in sensory cortex. Neuroscience 2002;111:709–38. [PubMed: 12031401]

Cant, NB.; Morest, DK. The structural basis for stimulus coding in the cochlear nucleus of the cat. In: Berlin, C., editor. Hearing Science: Recent Advances. San Diego, CA: College-Hill; 1984. p. 371-421.

Coleman JR, Clerici WJ. Sources of projections to subdivisions of the inferior colliculus in the rat. J Comp Neurol 1987;262:215–226. [PubMed: 3624552]

Davis KA, Ramachandran R, May BJ. Single-unit responses in the inferior colliculus of decerebrate cats. II. Sensitivity to interaural level differences. J Neurophysiol 1999;82:164–175. [PubMed: 10400945]

Davis KA. Evidence of a functionally segregated pathway from dorsal cochlear nucleus to inferior colliculus. J Neurophysiol 2002;87(4):1824–35. [PubMed: 11929904]

Davis KA, Ramachandran R, May BJ. Auditory processing of spectral cues for sound localization in the inferior colliculus. J Assoc Res Otolaryngol 2003;4:148–163. [PubMed: 12943370]

Ehret, G. The auditory midbrain, a “shunting yard” of acoustical information processing. In: Romand, R.; Ehret, G., editors. The Central Auditory System. New York: Oxford; 1997. p. 259-316.

Eggermont JJ, Komiya H. Moderate noise trauma in juvenile cats results in profound cortical topographic map changes in adulthood. Hear Res 2000;142:89–101. [PubMed: 10748332]

Frisina, RD.; Rajan, R. Inferior colliculus: Aging and plasticity. In: Winer, JA.; Schreiner, CE., editors. The Inferior Colliculus. New York: Springer; 2005. p. 559-584.

Harrison RV, Nagasawa A, Smith DW, Stanton S, Mount RJ. Reorganization of auditory cortex after neonatal high frequency cochlear hearing loss. Hear Res 1991;54:11–19. [PubMed: 1917710]

Harrison RV, Stanton S, Nagasawa A, Ibrahim D, Mount RJ. The effects of long-term cochlear hearing loss on the functional organization of central auditory pathways. J Otolaryngol 1993;22:4–11. [PubMed: 8445702]

Harrison RV, Stanton SG, Mount RJ. Effects of chronic cochlear damage on threshold and frequency tuning of neurons in AI auditory cortex. Acta Otolaryngol Suppl 1995;519:30–5. [PubMed: 7610889]

Harrison, RV.; Ibrahim, D.; Stanton, S.; Mount, RJ. Reorganization of frequency maps in Chinchilla auditory midbrain after long-term basal cochlear lesions induced at birth. In: Salvi, R.; Henderson, D.; Fiorino, F.; Colletti, V., editors. Auditory System Plasticity and Regeneration. New York: Thieme; 1996. p. 283-255.

Henkel CK. Axonal morphology in fibrodendritic laminae of the dorsal nucleus of the lateral lemniscus: afferent projections from the medial superior olivary nucleus. J Comp Neurol 1997;380:136–144. [PubMed: 9073088]

Henkel CK, Fuentes-Santamaria V, Alvarado JC, Brunso-Bechtold JK. Quantitative measurement of afferent layers in the ferret inferior colliculus. Hear Res 2003;177(1–2):32–42. [PubMed: 12618315]

Irvine DRF, Rajan R, McDermott HJ. Injury-induced reorganization in adult auditory cortex and its perceptual consequences. Hear Res 2000;147:188–199. [PubMed: 10962185]

Irvine DR, Rajan R, Smith S. Effects of restricted cochlear lesions in adult cats on the frequency organization of the inferior colliculus. J Comp Neurol 2003;467(3):354–74. [PubMed: 14608599]

Kaltenbach JA, Czaja J, Kaplan CR. Changes in the tonotopic map of the dorsal cochlear nucleus following induction of cochlear lesions by exposure to intense sound. Hear Res 1992;59:213–23. [PubMed: 1618712]

Kamke MR, Brown M, Irvine DRF. Plasticity in the tonotopic organization of the medial geniculate body in adult cats following restricted unilateral cochlear lesions. J Comp Neurol 2003;459:355–367. [PubMed: 12687704]

Kiang NY, Liberman MC, Levine RA. Auditory-nerve activity in cats exposed to ototoxic drugs and high-intensity sounds. Ann Otol Rhinol Laryngol 1976;85(6 PT 1):752–68. [PubMed: 999140]

Kimura M, Eggermont JJ. Effects of acute pure tone induced hearing loss on response properties in three auditory cortical fields in cat. Hear Res 1999;135(1–2):146–62. [PubMed: 10491963]

Kitzes LM, Semple MN. Single-unit responses in the inferior colliculus: Effects of neonatal unilateral cochlear ablation. J Neurophysiol 1985;53:1483–1500. [PubMed: 4009229]

Kitzes, LM. Anatomical and physiological changes in the brainstem induced by neonatal ablation of the cochlea. In: Salvi, R.; Henderson, D.; Fiorino, F.; Colletti, V., editors. Auditory System Plasticity and Regeneration. New York: Thieme; 1996. p. 256-274.

Kolarik RC, Rasey SK, Wall JT. The consistency, extent, and locations of early-onset changes in cortical nerve dominance aggregates following injury of nerves to primate hands. J Neurosci 1994;14(7): 4269–88. [PubMed: 8027778]

Krishna BS, Semple MN. Auditory temporal processing: responses to sinusoidally amplitude-modulated tones in the inferior colliculus. J Neurophysiol 2000;84(1):255–73. [PubMed: 10899201]

Lebeau FE, Malmierica MS, Rees A. Iontophoresis *In Vivo* Demonstrates a Key Role for GABAA and Glycinergic Inhibition in Shaping Frequency Response Areas in the Inferior Colliculus of Guinea Pig. J Neurosci 2001;21(18):7303–7312. [PubMed: 11549740]

Li H, Sabes JH, Sinex DG. Responses of Inferior Colliculus Neurons to SAM Tones Located in Inhibitory Response Areas. Hear Res 2006;220(1–2):116–125. [PubMed: 16945495]

Liberman MC, Kiang NY. Acoustic trauma in cats: Cochlear pathology and auditory-nerve activity. Acta Otolaryngol Suppl 1978;358:1–63. [PubMed: 281107]

Liberman, MC.; Mulroy, MJ. Acute and chronic effects of acoustic trauma: Cochlear pathology and auditory nerve pathophysiology. In: Hamernik, RP.; Henderson, D.; Salvi, R., editors. New Perspectives on Noise-Induced Hearing Loss. New York: Raven; 1982. p. 105-130.

Liberman MC, Dodds LW. Single-neuron and chronic cochlear pathology. II Stereocilia damage and alterations of spontaneous discharge rates. Hear Res 1984;16:43–53. [PubMed: 6511672]

Malmierca MS, Rees A, Le Beau FE, Bjaalie JG. Laminar organization of frequency-defined local axons within and between the inferior colliculi of the guinea pig. J Comp Neurol 1995;357:124–144. [PubMed: 7673462]

Malmierca MS, Saint Marie RL, Merchan M, Oliver DL. Laminar inputs from dorsal cochlear nucleus and ventral cochlear nucleus to the central nucleus of the inferior colliculus: Two patterns of convergence. Neuroscience 2005;136(3):883–94. [PubMed: 16344158]

Nataraj K, Wenstrup JJ. Roles of inhibition in complex auditory responses in the inferior colliculus: inhibited combination-sensitive neurons. J Neurophysiol 2006;95(4):2179–92. [PubMed: 16371455]

Nataraj K, Wenstrup JJ. Roles of inhibition in creating complex auditory responses in the inferior colliculus: facilitated combination-sensitive neurons. J Neurophysiol 2005;93(6):3294–312. [PubMed: 15689388]

Noreña AJ, Tomita M, Eggermont JJ. Neural changes in cat auditory cortex after a transient pure-tone trauma. J Neurophysiol 2003;90(4):2387–401. [PubMed: 12773493]

Oliver DL. Projections to the inferior colliculus from the anteroventral cochlear nucleus in the cat: Possible substrates for binaural interaction. J Comp Neurol 1987;264:24–46. [PubMed: 2445792]

Oliver, DL.; Shneiderman, A. The anatomy of the inferior colliculus: A cellular basis for integration of monaural and binaural information. In: Altschuler, RA.; Bobbin, RP.; Clopton, BM.; Hoffman, DW., editors. Neurobiology of Hearing: The Central Auditory System. New York: Raven Press; 1991. p. 195-222.

Oliver, DL.; Beckius, GE. Ascending projections from the cochlear nucleus to the inferior colliculus and their interactions with projections from the superior olivary complex. In: Merchán, MA.; Juiz, JM.; Godfrey, DA.; Mugnaini, E., editors. The Mammalian Cochlear Nuclei: Organization and Function. Plenum Press; New York: 1993. p. 335-347.

Oliver DL, Beckius GE, Shneiderman A. Axonal projections from the lateral and medial superior olive to the inferior colliculus of the cat: A study using electron microscopic autoradiography. J Comp Neurol 1995;360:17–32. [PubMed: 7499562]

Oliver DL, Beckius GE, Bishop DC, Kuwada S. Simultaneous anterograde labeling of axonal layers from lateral superior olive and dorsal cochlear nucleus in the inferior colliculus of cat. J Comp Neurol 1997;382(2):215–29. [PubMed: 9183690]

Osen KK. Projection of the cochlear nuclei on the inferior colliculus in the cat. J Comp Neurol 1972;144:355–372. [PubMed: 5027335]

Palmer CV, Nelson CT, Lindley GA. The functionally and physiologically plastic adult auditory system. J Acoust Soc Am 1998;103:1705–1721. [PubMed: 9566316]

Portfors CV, Wenstrup JJ. Excitatory and facilitatory frequency response areas in the inferior colliculus of the mustached bat. Hear Res 2002;168(1–2):131–8. [PubMed: 12117515]

Rajan R. Receptor organ damage causes loss of cortical surround inhibition without topographic map plasticity. Nature Neurosci 1998;1:138–143. [PubMed: 10195129]

Rajan R, Irvine DRF, Wise LZ, Heil P. Effects of unilateral partial cochlear lesions in adult cats on the representation of lesioned and unlesioned cochleas in primary auditory cortex. J Comp Neurol 1993;338:17–49. [PubMed: 8300898]

Rajan, R.; Irvine, DRF. Features of, and boundry conditions for, lesion-induced reorganization of adult auditory cortical maps. In: Salvi, R.; Henderson, D.; Fiorino, F.; Colletti, V., editors. Auditory System Plasticity and Regeneration. New York: Thieme; 1996. p. 224-237.

Rajan R, Irvine DRF. Neuronal responses across cortical field AI in plasticity induced by peripheral auditory organ damage. Audiol Neuro-Otol 1998a;3:123–144.

Rajan R, Irvine DRF. Absence of plasticity of the frequency map in dorsal cochlear nucleus of adult cats after unilateral partial cochlear lesions. J Comp Neurol 1998b;399:35–46. [PubMed: 9725699]

Ramachandran R, Davis KA, May BJ. Single-unit responses in the inferior colliculus of decerebrate cats. I Classification based on frequency response maps. J Neurophysiol 1999;82:152–163. [PubMed: 10400944]

Reale RA, Brugge JF, Chan JCK. Maps of auditory cortex in cats after unilateral cochlear ablation in the neonatal period. Devel Brain Res 1987;34:281–290.

Rees A, Palmer AR. Neuronal responses to amplitude-modulated and pure-tone stimuli in the guinea pig inferior colliculus, and their modification by broadband noise. J Acoust Soc Am 1989;85(5):1978–1994. [PubMed: 2732379]

Rhode, WS. Physiological-morphological properties of the cochlear nucleus. In: Altschuler, RA.; Bobbin, PB.; Clopton, BM.; Hoffman, DW., editors. Neurobiology of Hearing: The Central Auditory System. New York: Raven; 1991. p. 47-77.

Rose JE, Greenwood DD, Goldberg JM, Hind JE. Some discharge characteristics of single neurons in the inferior colliculus of the cat. I. Tonotopical organization, relation to spike-sounds to tone intensity, and firing patterns of single elements. J Neurophysiol 1963;26(2):294–320.

Robertson D. Effects of acoustic trauma on stereocilia structure and spiral ganglion cell tuning properties in the guinea pig cochlea. Hear Res 1982;7(1):55–74. [PubMed: 7096217]

Robertson D, Irvine DRF. Plasticity of frequency organization in auditory cortex of guinea pig with partial unilateral deafness. J Comp Neurol 1989;282:456–471. [PubMed: 2715393]

Ryan A, Miller J. Single unit responses in the inferior colliculus of the awake and performing rhesus monkey. Exp Brain Res 1978;32(3):389–407. [PubMed: 98341]

Salvi R, Hamernik RP, Henderson D. Response patterns of auditory nerve fibers during temporary threshold shift. Hear Res 1982;10:37–67. [PubMed: 6841278]

Salvi, RJ.; Wang, J.; Powers, N. Rapid functional reorganization in the inferior colliculus and cochlear nucleus after acute cochlear damage. In: Salvi, R.; Henderson, D.; Fiorino, F.; Colletti, V., editors. Auditory System Plasticity and Regeneration. New York: Thieme; 1996. p. 275-296.

Schmid LM, Rosa MG, Calford MB. Retinal detachment induces massive immediate reorganization in visual cortex. Neuroreport 1995;6(9):1349–53. [PubMed: 7670002]

Scholes C, Snyder RL, Sumner C. Modelling excitatory and inhibitory convergence in the inferior colliculus (IC): receptive field plasticity. Assoc for Res in Otolaryngol Abastract. 2006

Schreiner CE, Langner G. Periodicity coding in the inferior colliculus of the cat. II Topographical organization. J Neurophysiol 1988;60:1823–1840. [PubMed: 3236053]

Seki S, Eggermont JJ. Changes in cat primary auditory cortex after minor-to-moderate pure-tone induced hearing loss. Hear Res 2002;173(1–2):172–86. [PubMed: 12372645]

Semple MN, Aitkin LM. Representation of sound frequency and laterality by units in central nucleus of cat inferior colliculus. J Neurophysiol 1979;42(6):1626–39. [PubMed: 501392]

Serviere J, Webster WR, Calford MB. Isofrequency labeling revealed by a combined [14C]-2-deoxyglucose, electrophysiological, and horseradish peroxidase study of the inferior colliculus of the cat. J Comp Neurol 1984;228(4):463–77. [PubMed: 6490965]

Servière J, Webster WR. A combined electrophysiological and [14C] 2-deoxyglucose study of the frequency organization of the inferior colliculus of the cat. Neurosci Lett 1981;27(2):113–8. [PubMed: 7322445]

Shaffer LA, Withnell RH, Dhar S, Lilly DJ, Goodman SS, Harmon KM. Sources and mechanisms of DPOAE generation: implications for the prediction of auditory sensitivity. Ear Hear 2003;24(5):367–379. [PubMed: 14534408]

Seki S, Eggermont JJ. Changes in cat primary auditory cortex after minor-to-moderate pure-tone induced hearing loss. Hear Res 2002;173(1–2):172–86. [PubMed: 12372645]

Sinex DG. Responses of cochlear nucleus neurons to harmonic and mistuned complex tones. Hear Res 2008;238(1–2):39–48. [PubMed: 18078726]

Sinex DG. Spectral processing and sound source determination. Int Rev Neurobiol 2005;70:371–98. [PubMed: 16472640]

Sinex DG, Guzik H, Li H, Henderson-Sabes J. Responses of auditory nerve fibers to harmonic and mistuned complex tones. Hear Res 2003;182(1–2):130–9. [PubMed: 12948608]

Sinex DG, Li H. Responses of inferior colliculus neurons to double harmonic tones. J Neurophysiol 2007;98(6):3171–84. [PubMed: 17913991]

Sinex DG, Sabes JH, Li H. Responses of inferior colliculus neurons to harmonic and mistuned complex tones. Hear Res 2002;168(1–2):150–62. [PubMed: 12117517]

Snyder RL, Sinex DG, McGee JD, Walsh EJ. Acute spiral ganglion lesions change the tuning and tonotopic organization of cat inferior colliculus neurons. Hear Res 2000;147:221–241. [PubMed: 10962187]

Snyder RL, Sinex DG. Tonotopic reorganization of cat primary auditory cortex after acute lesions of restricted sectors of the spiral ganglion. Soc for Neurosci (Abs). 1998

Snyder RL, Sinex DG. Immediate changes in the tuning properties of cat inferior colliculus (IC) neurons recorded with fixed in-dwelling electrodes. Assoc Res Otolaryngol 2002;23:258.

Suga N, Tsuzuki K. Inhibition and level-tolerant frequency tuning in the auditory cortex of the mustached bat. J Neurophysiol 1985;53:1109–1145. [PubMed: 3998795]

Sumner CJ, Scholes C, Snyder RL. Re-tuning of inferior colliculus neurons following spiral ganglion lesions: a single neuron model of converging inputs. J Assoc Res Otol. 200810.1007/s10162-008-0139-6

Syka J. Plastic changes in the central auditory system after hearing loss, restoration of function, and during learning. Physiol Rev 2002;82:601–636. [PubMed: 12087130]

Tierney TS, Russell FA, Moore DR. Susceptibility of developing cochlear nucleus neurons to deafferentation-induced death abruptly ends just before the onset of hearing. J Comp Neurol 1997;378:295–306. [PubMed: 9120067]

Wang J, Salvi RJ, Powers N. Plasticity of response properties of inferior colliculus neurons following acute cochlear damage. J Neurophysiol 1996;75:171–183. [PubMed: 8822550]

Webster WR, Servière J, Batini C, Laplante S. Autoradiographic demonstration with 2-[^{14}C] deoxyglucose of frequency selectivity in the auditory system of cats under conditions of functional activity. Neurosci Lett 1978;10:43–48.

Weinberger NM. Dynamic regulation of receptive fields and maps in the adult sensory cortex. Ann Rev Neurosci 1995;18:129–158. [PubMed: 7605058]

Whitley JM, Henkel CK. Topographical organization of the inferior collicular projection and other connections of the ventral nucleus of the lateral lemniscus in the cat. J Comp Neurol 1984;229:257–270. [PubMed: 6501602]

Willott JF. Changes in frequency representation in the auditory system of mice with age related hearing impairment. Brain Res 1984;309:159–162. [PubMed: 6488006]

Willott JF, Aitkin LM, McFadden SM. Plasticity of auditory cortex associated with sensorineural hearing loss in adult C57BL/6J mice. J Comp Neurol 1993;329:402–411. [PubMed: 8459051]

Willott, JF. Auditory system Plasticity in the adult C57BL/6J mouse. In: Salvi, R.; Henderson, D.; Fiorino, F.; Colletti, V., editors. Auditory System Plasticity and Regeneration. New York: Thieme; 1996. p. 297-316.

Xie R, Gittelman JX, Pollak GD. Rethinking tuning: in vivo whole-cell recordings of the inferior colliculus in awake bats. J Neurosci 2007;27(35):9469–81. [PubMed: 17728460]

Yang L, Pollak GD, Resler C. GABAergic circuits sharpen tuning curves and modify response properties in the mustache bat inferior colliculus. J Neurophysiol 1992;68:1760–1774. [PubMed: 1479443]

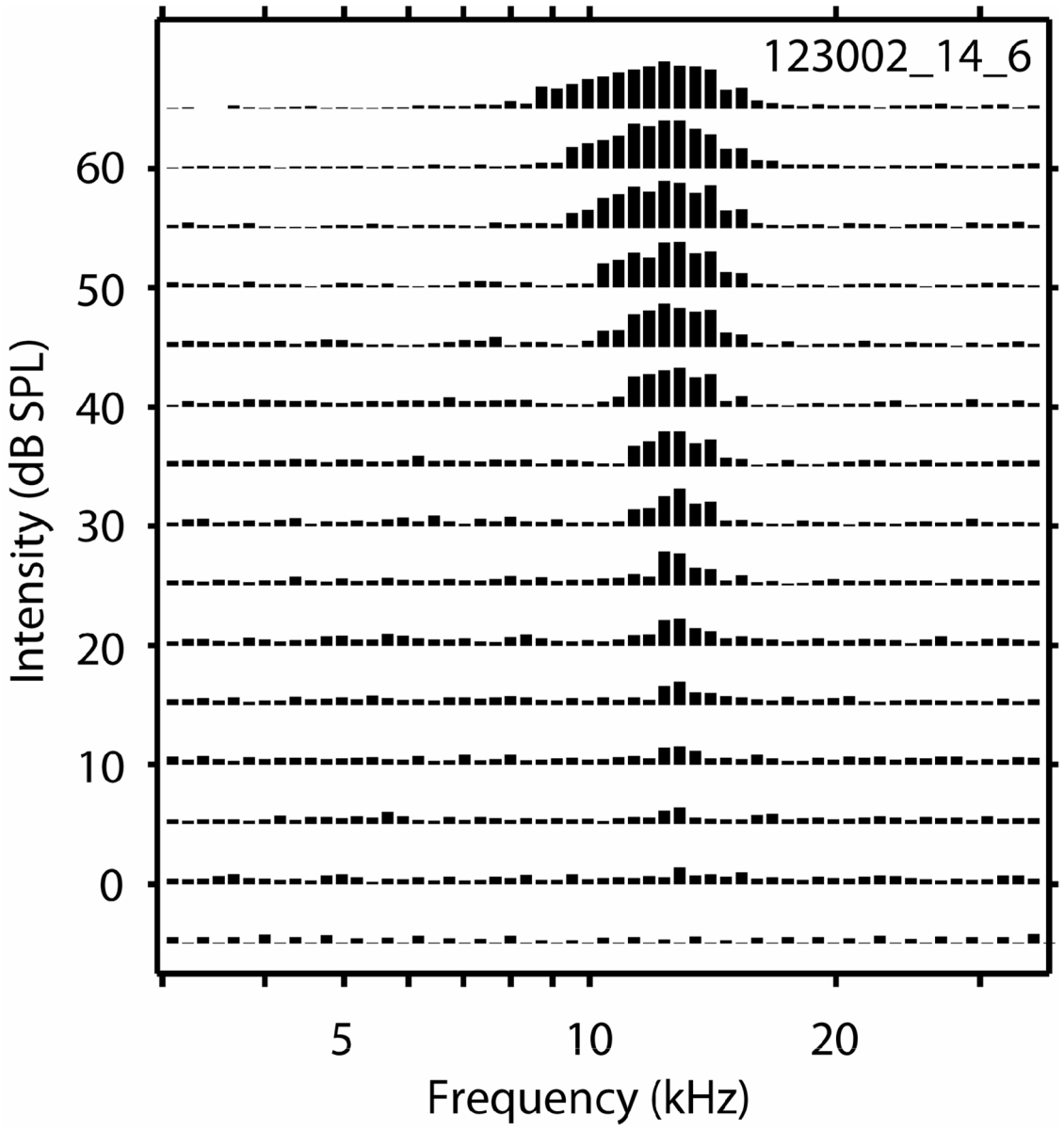

Figure 1.
An example of an ICC frequency response area. Response amplitude to each stimulus frequency/intensity pair is normalized to the maximum response and plotted as a vertical bar.

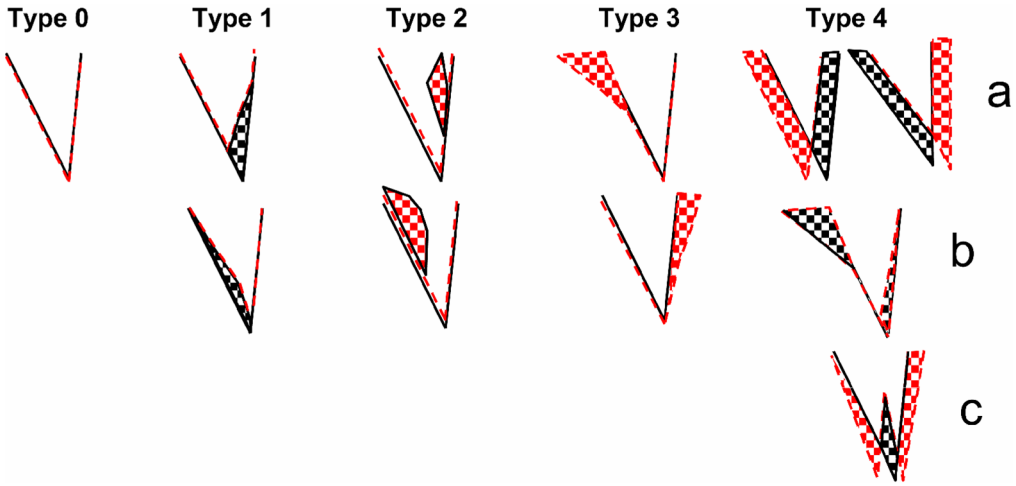

Figure 2.
Illustration of the 5 categories of post-lesion FRA changes observed after relatively large final cochlear lesions. The black lines indicate the pre-lesion threshold tuning curves, red dashed lines indicate the post-lesion threshold tuning curves, checkered areas indicate regions of post-lesion increases (red) and losses (black) in excitation relative to pre-lesion responses.

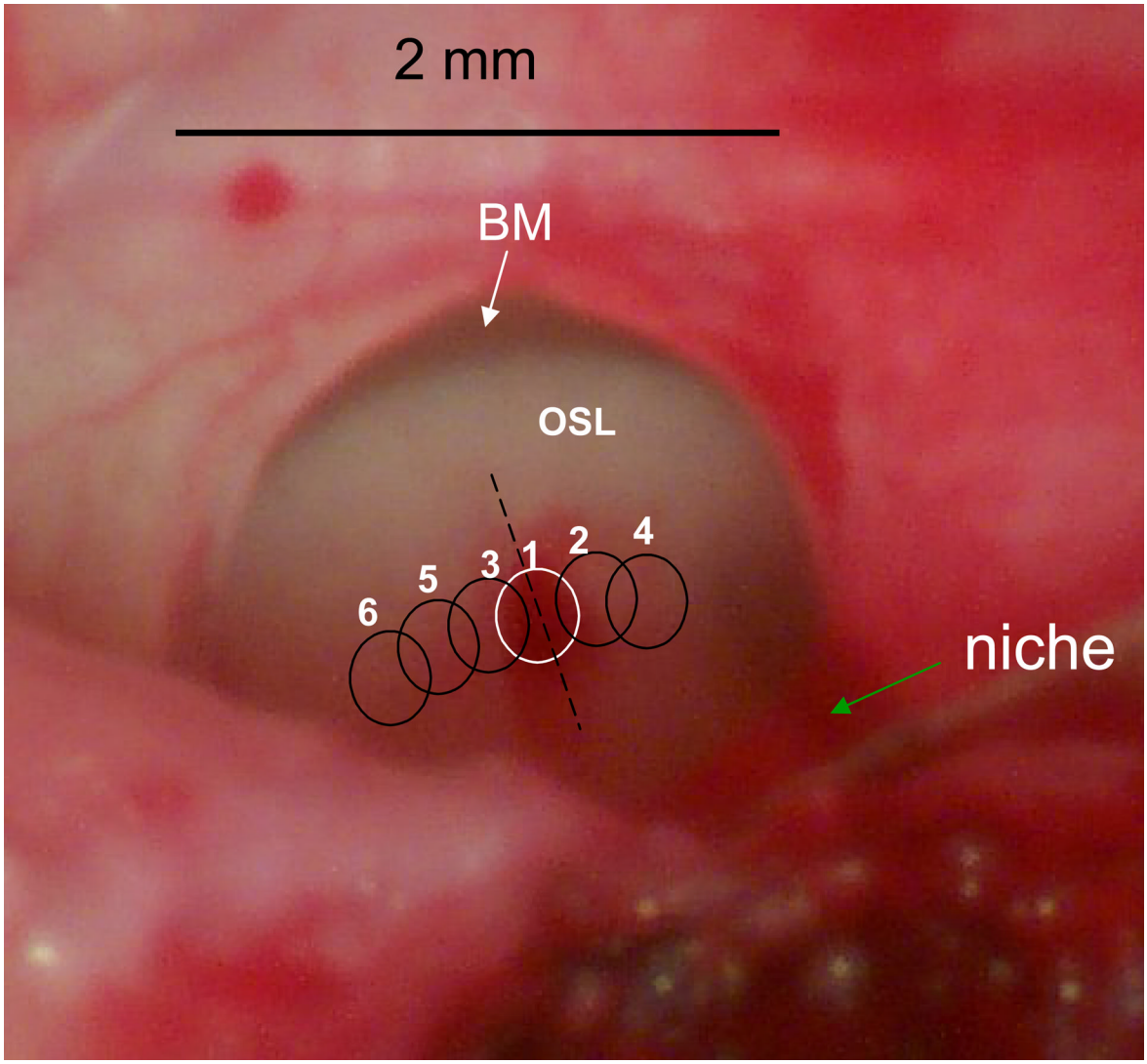

Figure 3.
View through the round window into hook region the cat cochlea. In this preparation the round window membrane has been completely removed and all perilymph has been drained from the scala tympani. The osseous spiral lamina (OSL) and the basilar membrane (BM, white arrow) can be seen. Prior to taking this photo, Rosenthal's canal was irradiated with high energy 2.5 mJ/pulse pulses for 5 seconds (10 pps). This intentionally high level exposure produced a lesion which is outlined by the white circle #1. This lesion is larger and deeper than our standard lesions, but it is more easily visualized. The site of the lesion can be identified by the presence of extravasated blood, a feature rarely seen after standard lesions. Subsequent overlapping lesions are indicated by black circles 2 – 6.

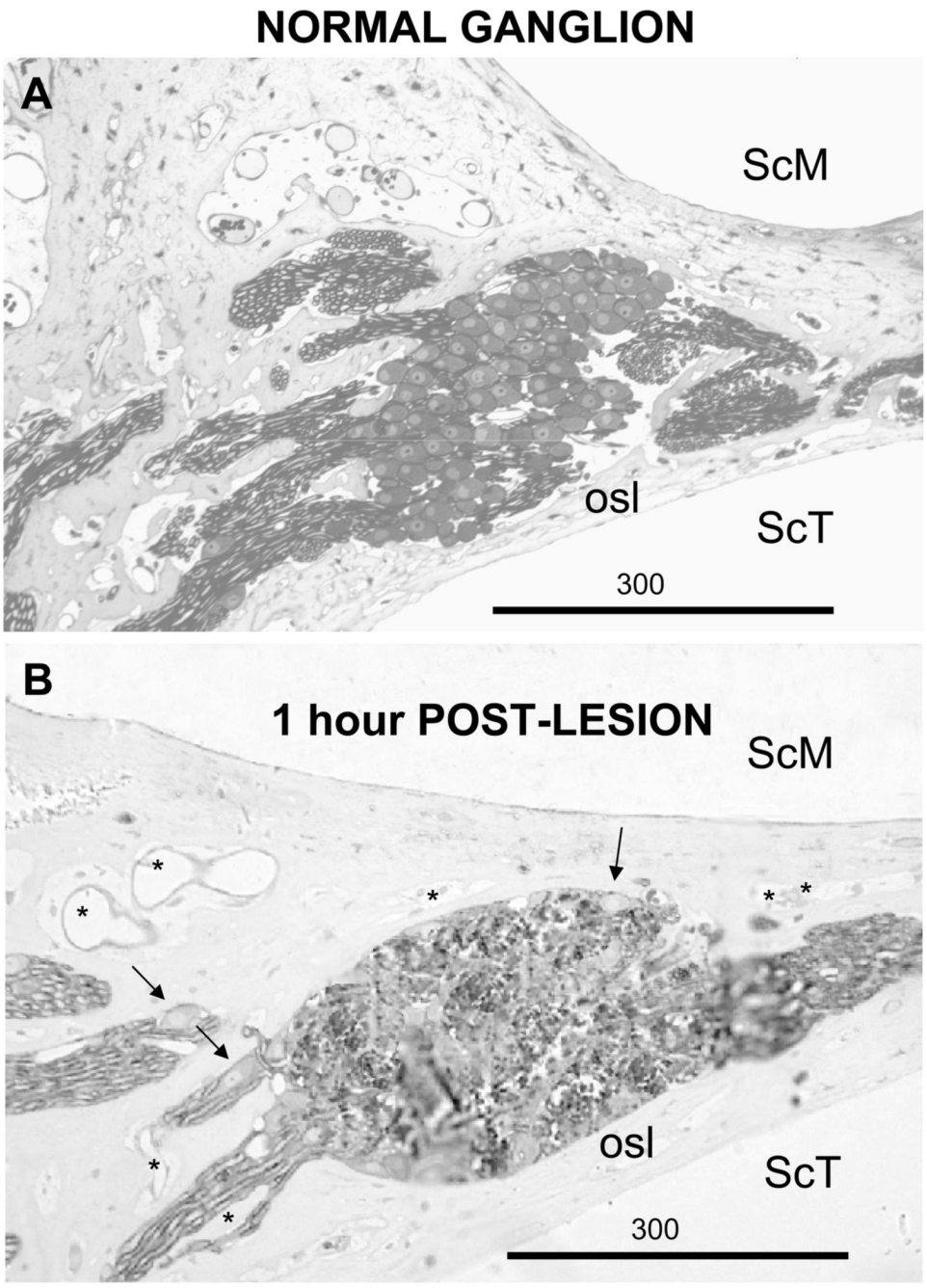

Figure 4.

A. Radial section through the osseous spiral lamina (osl) and Rosenthal's canal in of an intact cat. The scala media (SCM) is toward the top and the scala tympani (ScT) is toward the bottom. The modiolus is toward the left and the organ of Corti is toward the right. B. A similar section through a laser lesion of the ganglion at a level similar to the dashed line in Figure 3. Rosenthal's canal was irradiated with 1.5 mJ/pulses at 10 pps for 5 sec. 1 hour later the cochlea was fixed by intrascalar perfusion. The arrows indicate intact spiral ganglion cells at the periphery of the lesion (K614). Asterisks indicate intact blood vessels.

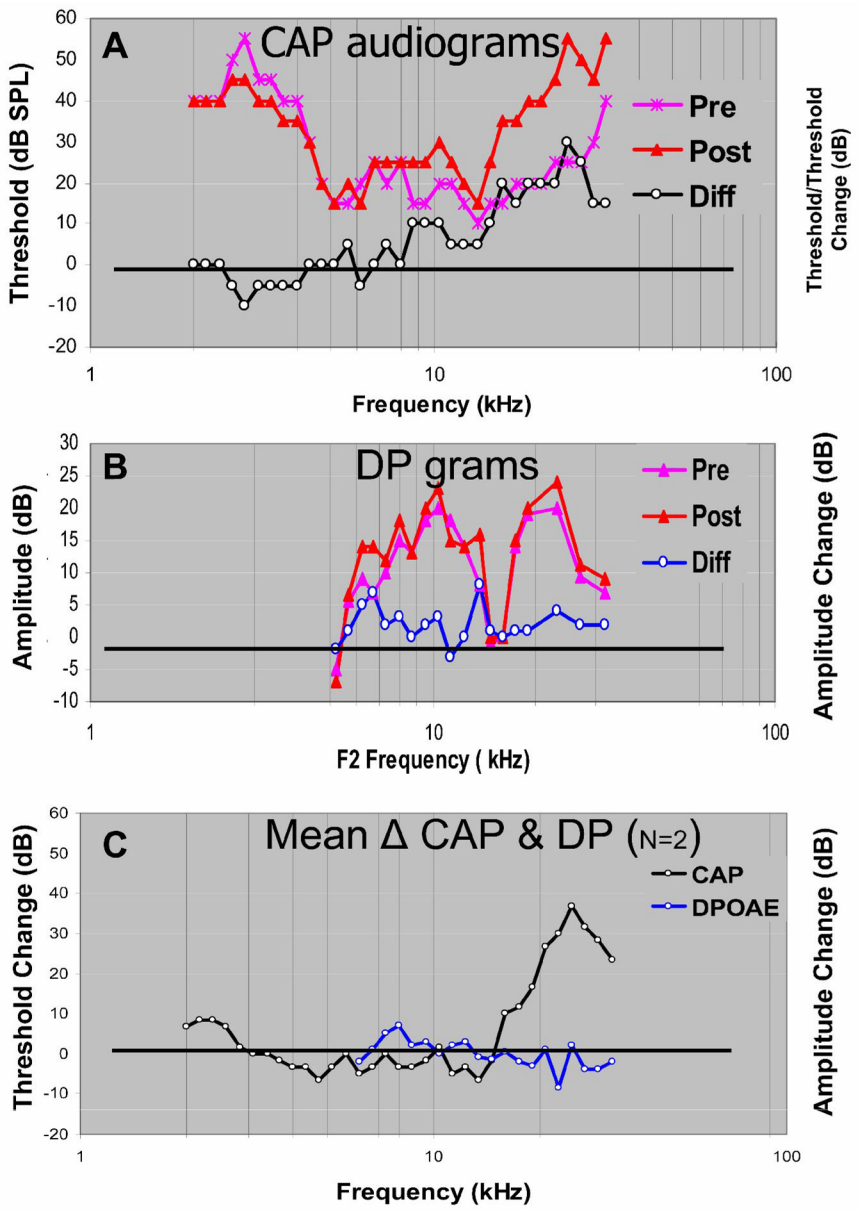

Figure 5.

A. Tone-evoked CAP threshold audiograms. Pre-lesion (asterisks), post-lesion (triangles) and difference (circles) audiograms are shown from one cat (L064). Pre- and Post-lesion thresholds are displayed in dB SPL. The difference levels are displayed in dB SL (post-lesion minus pre-lesion thresholds). B. DP-grams from the same animal. The distortion product amplitudes as a function of F2 frequency plotted in dB SPL and differences (post-lesion minus pre-lesion) in dB re pre-lesion thresholds. C. Average change in CAP threshold and 2F1-F2 distortion product amplitude as a function of F2 frequency for lesions in 2 cats (L064 and L075), in which LCFs were 25 kHz.

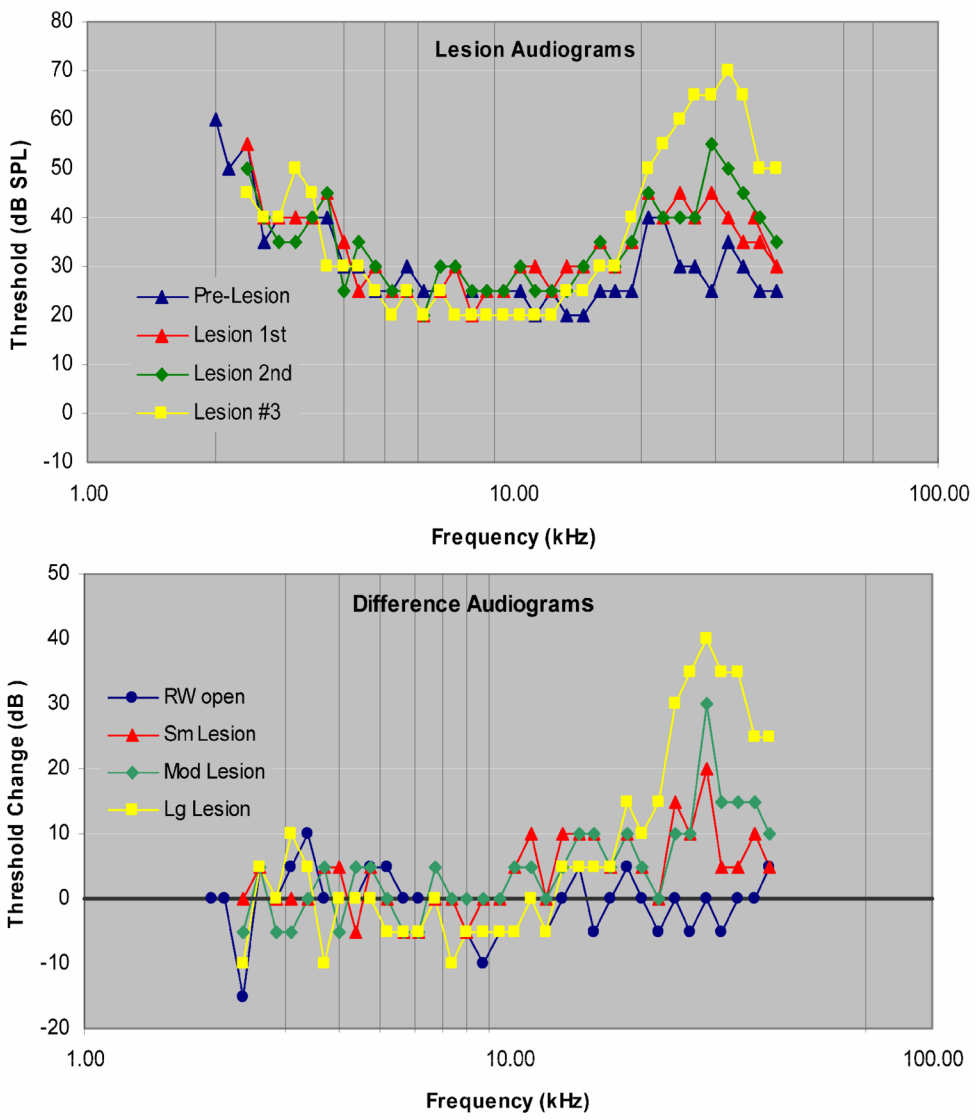

Figure 6.

A. CAP audiograms recorded after the round window was opened and after 3 progressively enlarged SG-lesions in animal 123002. B. Difference (post-lesion minus pre-lesion threshold) audiograms. LCF as indicated by the audiograms is estimated to be 29 kHz. The black horizontal line indicates pre-lesion CAP threshold.

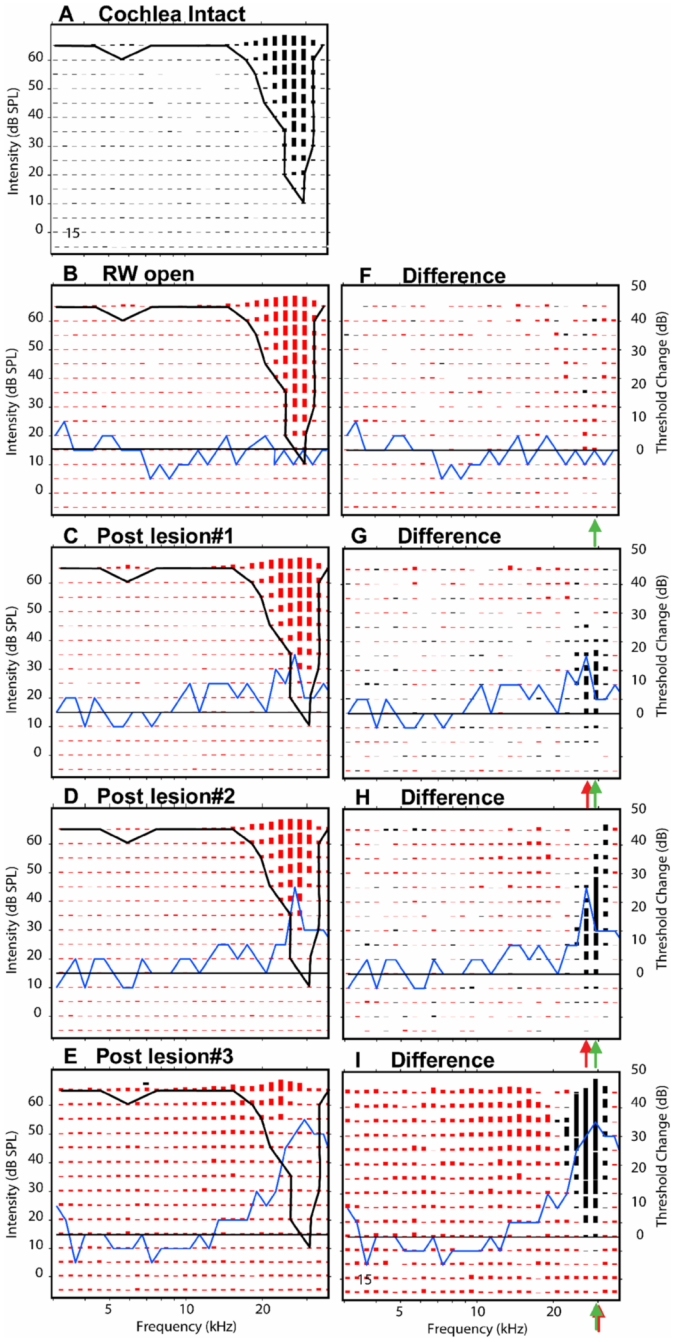

Figure 7.

Response areas recorded at one recording site in the ICC (#15, CF=28 kHz) showing the effects of three successively larger SG lesions. On the left column, panels show the response areas at 5 successive experimental stages: cochlea intact (A), after the round window has been opened (B) and then after three successively larger SG lesion responses (C–E). The black curve in each of these panels indicates the threshold tuning curve of the control responses. The blue curves indicate the changes (post-lesion minus control) in CAP thresholds at each experimental stage; the black horizontal line indicates no change in CAP threshold. Panels in the right column show the differences in response amplitude between control and post-lesion responses. Losses of excitation (round window open amplitudes > post-lesion amplitudes) are plotted in black;

post-lesion gains in excitation are plotted in red. Successive horizontal pairs of panels (B–F, C–G, D–H, and E–I) represents the responses at successively experimental stages. Red arrows indicate estimates of the frequency at which the largest loss in excitation occurred. Green arrows indicate pre-lesion CF. Asterisks in the difference plots indicate frequency/level combinations where excitatory response amplitudes were unaffected by the lesion.

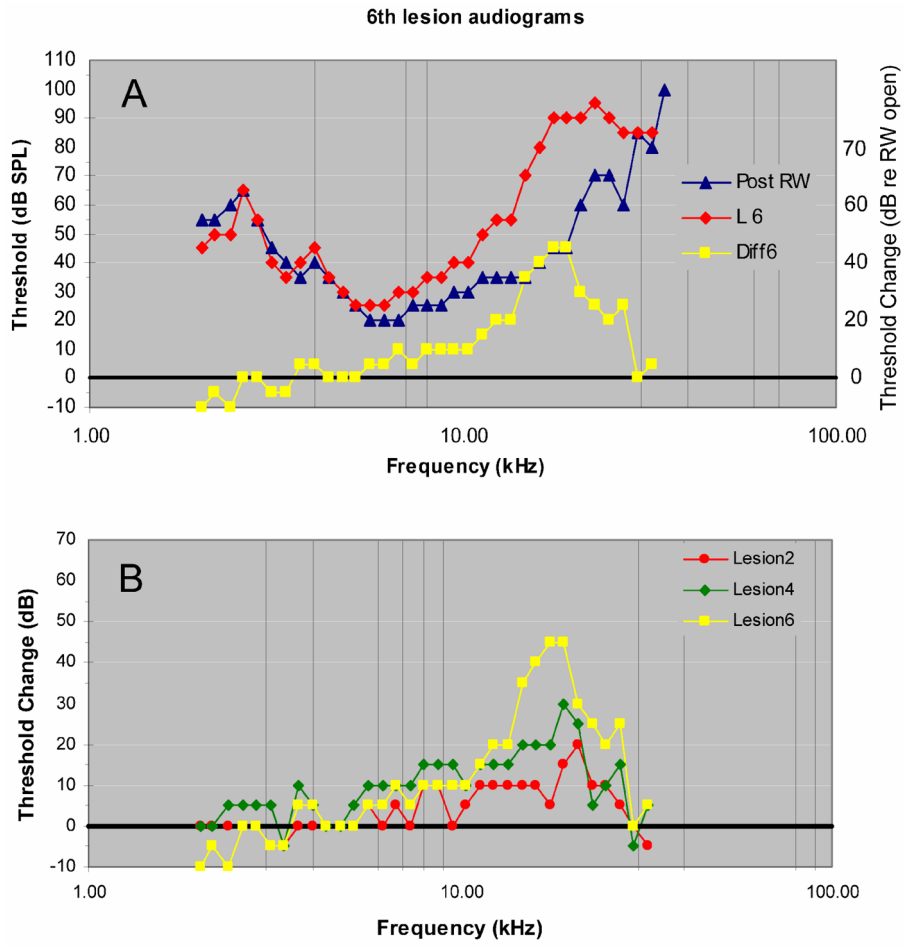

Figure 8.

A. Pre-, Post-lesion and Difference (post-lesion minus pre-lesion) audiograms recorded after the 6th and largest lesion in animal K435. B. Difference audiograms after the 2nd, 4th and 6th lesions.

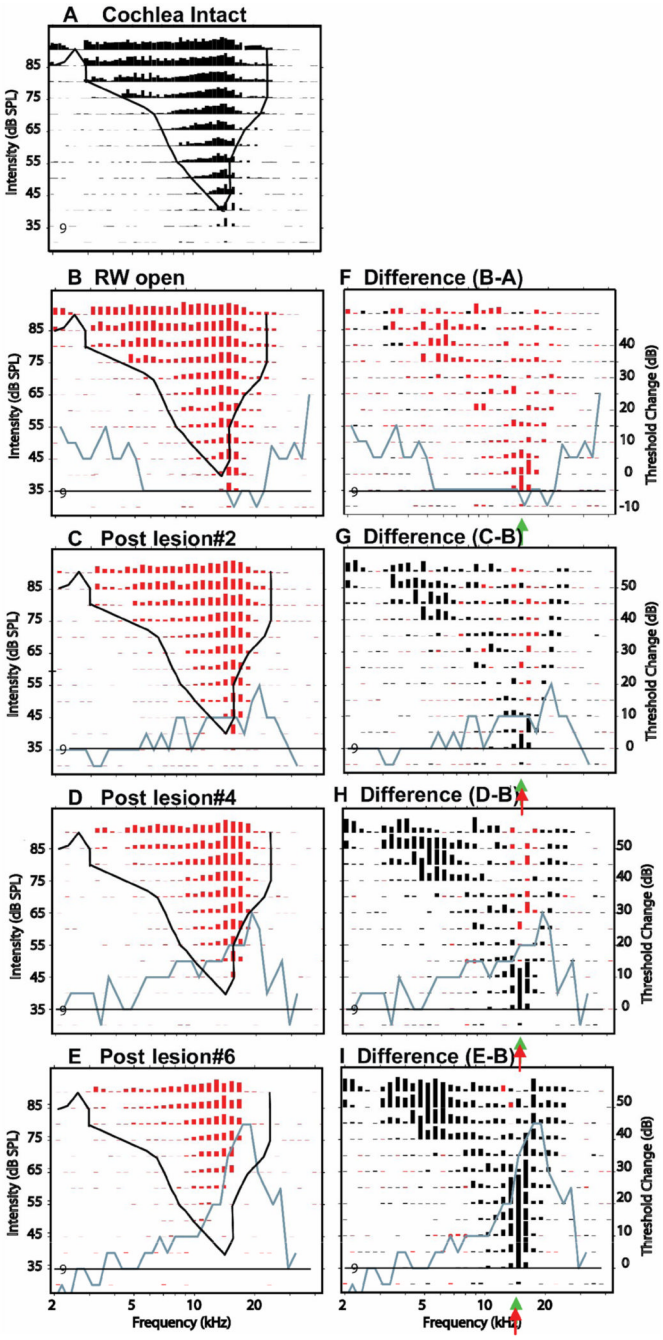

Figure 9.

Effects of 3 successively larger SG-lesions at a site #9 located at 800 mm from the most superficial site. CF & BF = 14.7 kHz. The left column of panels show response areas at 5 successive experimental stages: cochlea intact (A), after the round window has been opened (B) and then after three successively larger SG-lesions (C–E). Black curve in each panel is the threshold tuning curve of responses in the intact cochlea. Blue curves plot CAP thresholds changes (post-lesion minus control) at each experimental stage; Black horizontal line plots the no-change contour in CAP threshold. The right column of panels shows the differences in response amplitudes between control (B) and post-lesion responses at each stage. Post-lesion excitatory losses (round window open amplitudes > post-lesion amplitudes) are plotted in

black; post-lesion excitatory gains are plotted in red. Red arrows indicate estimates of the frequency at which the largest loss in excitation occurred. Green arrows indicate pre-lesion CF. Black slanted arrows indicate excitatory losses in low frequency response “tails” at frequencies remote from the lesion frequencies.

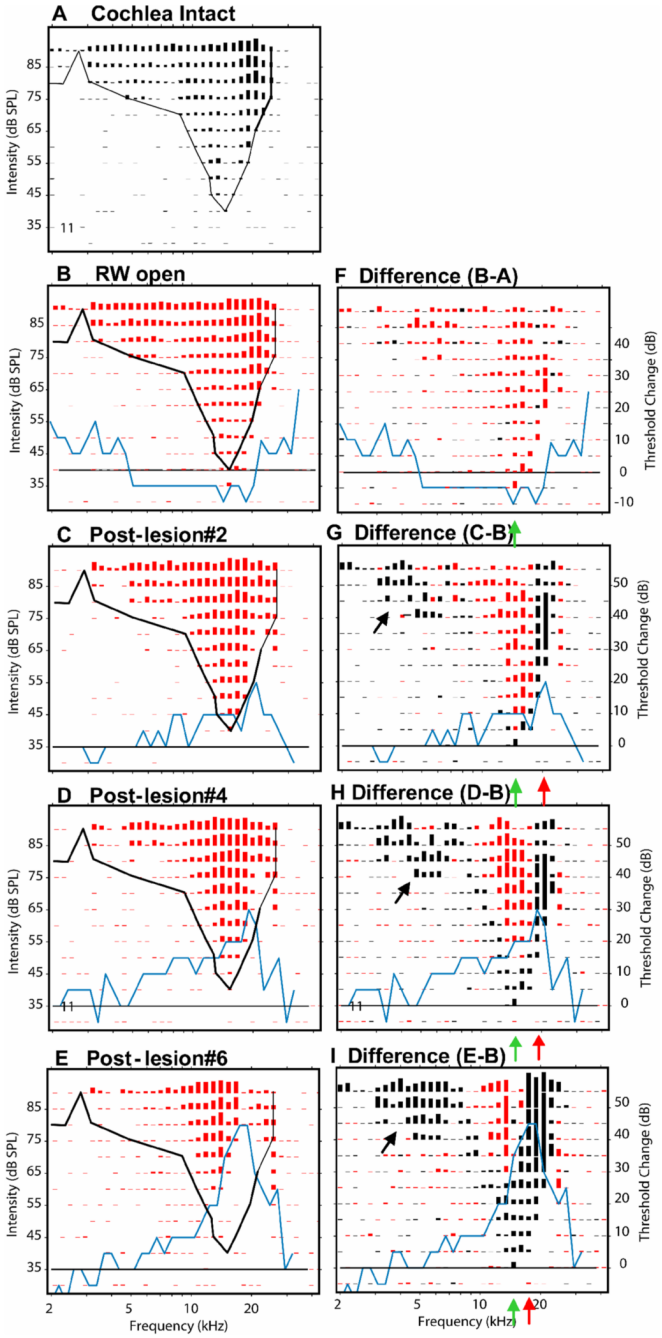

Figure 10.

Effects of the same 3 successively larger SG-lesions as shown in Fig. 9. This site is 200 um deeper in the ICC than site #9 with CF = 14.6 kHz and BF = 20.8 kHz. Asterisks indicate apex of the lesion-induced notch in excitatory region.

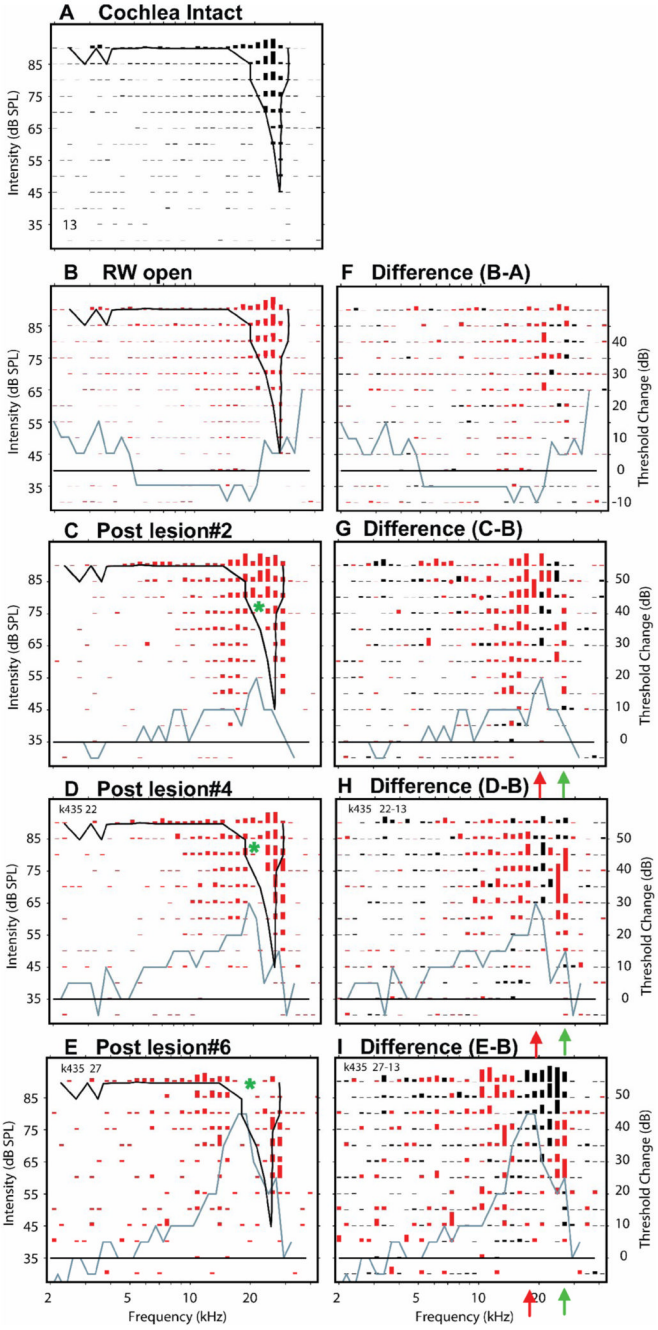

Figure 11.

Effects of same successively larger SG-lesions at site #13 which is 200 um deeper than the site in Fig. 10 with CF = 27 kHz, BF = 24 kHz. Asterisks indicate apex of the lesion-induced notches in the excitatory regions.

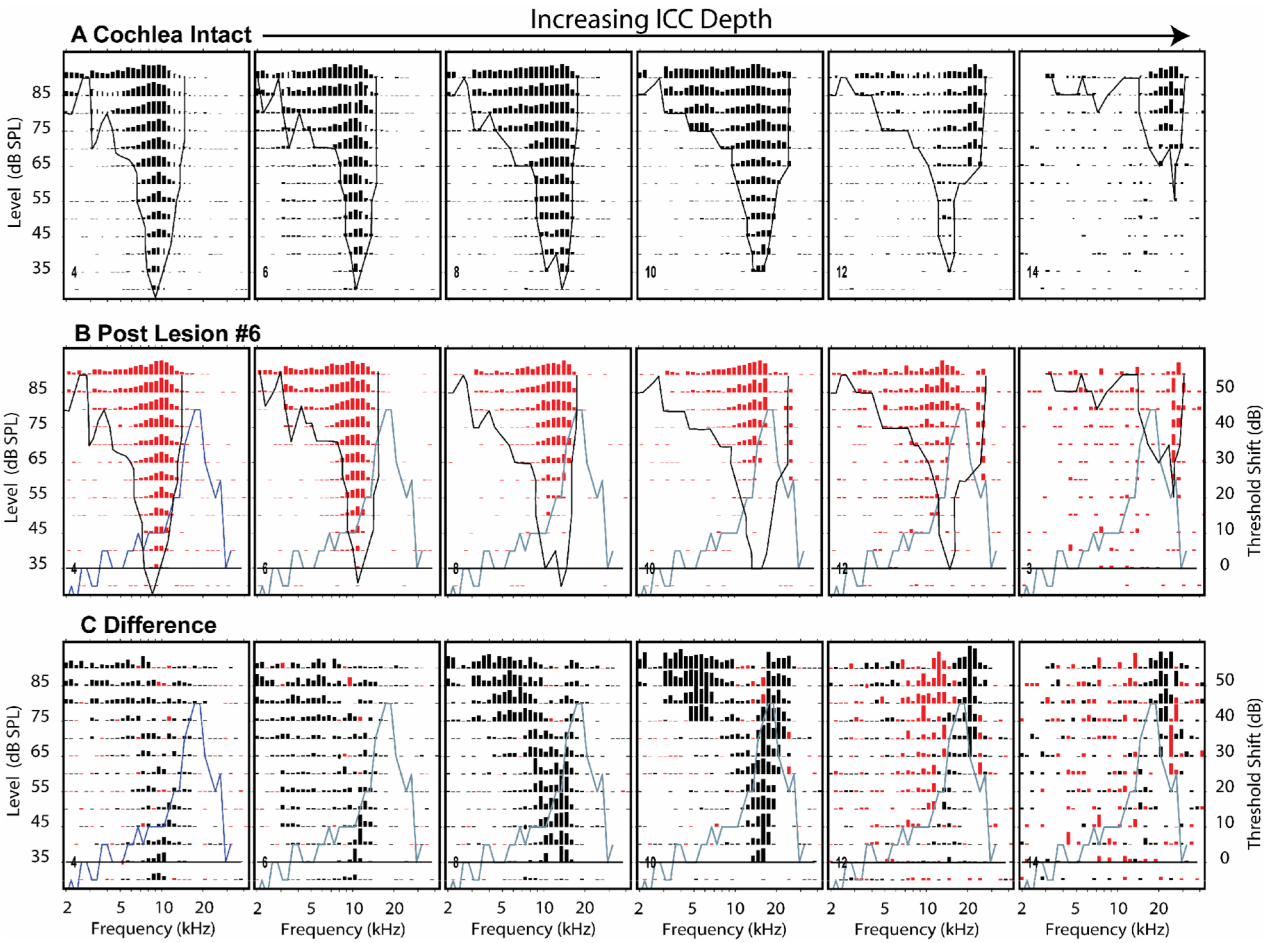

Figure 12.

Effects of a single, large lesion on response areas measured at 6 of 16 probe sites in one animal, k435A. The recording sites were distributed along the tonotopic axis of the ICC and separated by 200 microns with the most superficial site (#4) on the left, and the deepest site (#14) on the right. (A.) Pre-lesion responses. Each panel illustrates a pre-lesion FRA from one probe recording site. In this experiment CFs ranged from 6 to 26 kHz. The format of each panel is similar to those in Figure 6. (B.) Post-lesion responses at the same sites. The black curves in A and B indicate the pre-lesion threshold tuning curves. The blue curves indicate the CAP difference audiogram. The horizontal line indicates zero change in CAP threshold. (C.) Difference response areas comparable to those in Figure 6. Black lines represent post-lesion losses of excitation; red lines represent post-lesion excitation gains.

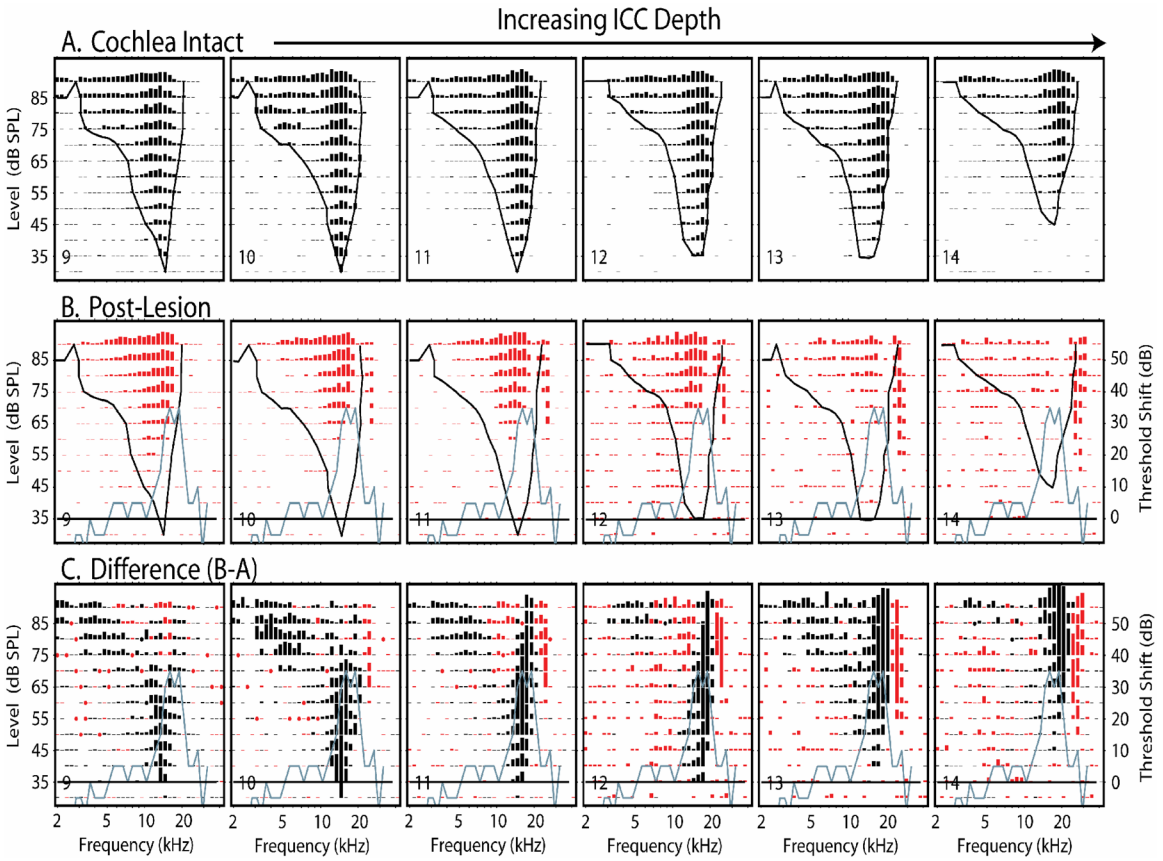

Figure 13.

The effects of a single spiral ganglion lesion on the responses recorded at 6 consecutive sites distributed along the tontotopic axis of the ICC in one animal, k345B after a large lesion (#6). The sites are separated by 100 μm. The format of this figure is similar to that of Figure 11. (A) Pre-lesion response areas. (B) Post-lesion response areas recorded from the same sites. (C) Difference response areas (post-lesion minus pre-lesion). Note the consistent gain of excitation at frequencies on the high frequency edge of the lesion frequencies (blue curve).

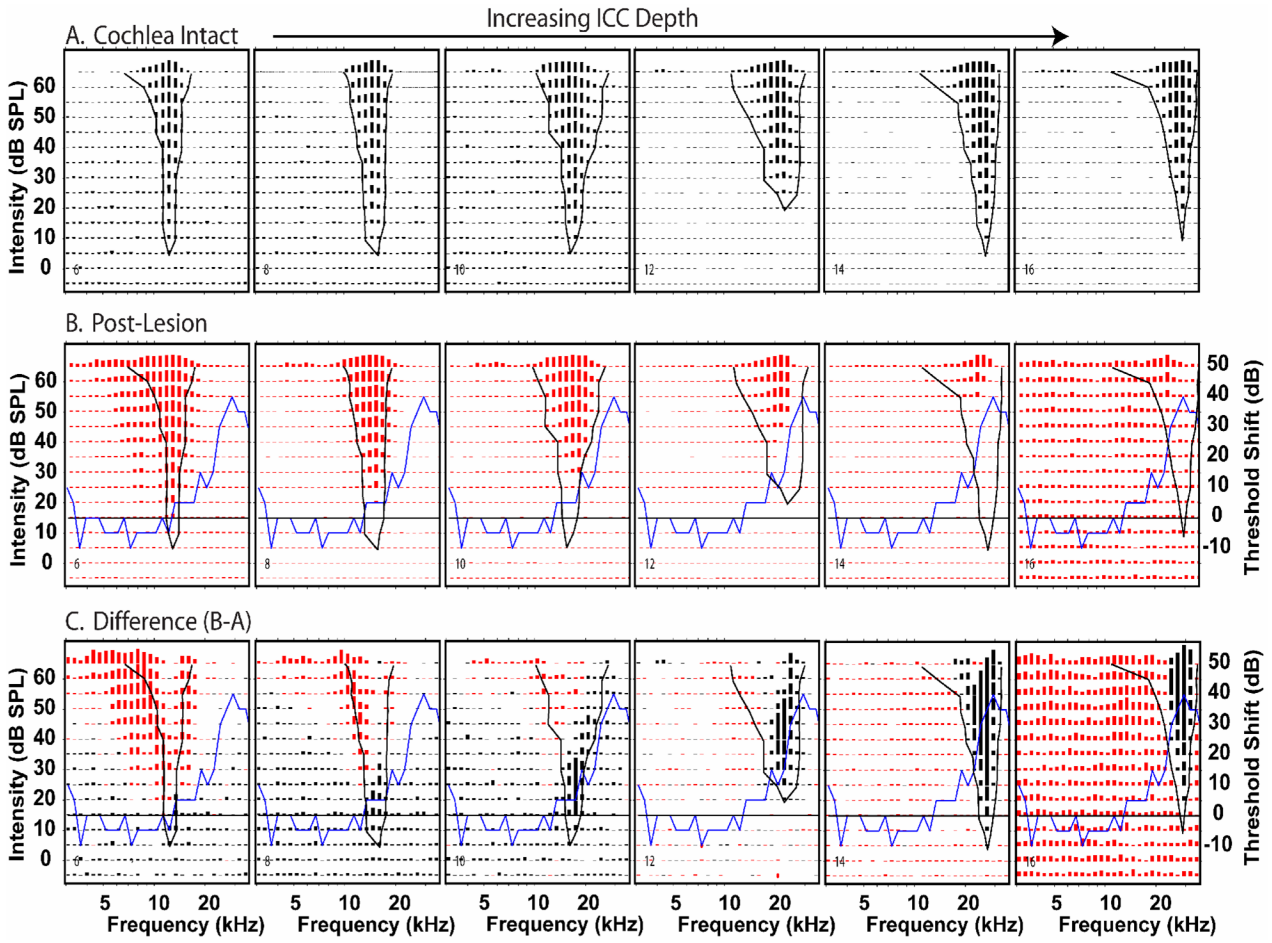

Figure 14.

Effects of a single, large lesion on response areas measured at 6 of 16 probe sites in one animal, 123002 The format of this figure is similar to that in Figure 11. (A.) Pre-lesion responses. (B.) Post-lesion responses. (C.) Difference response areas

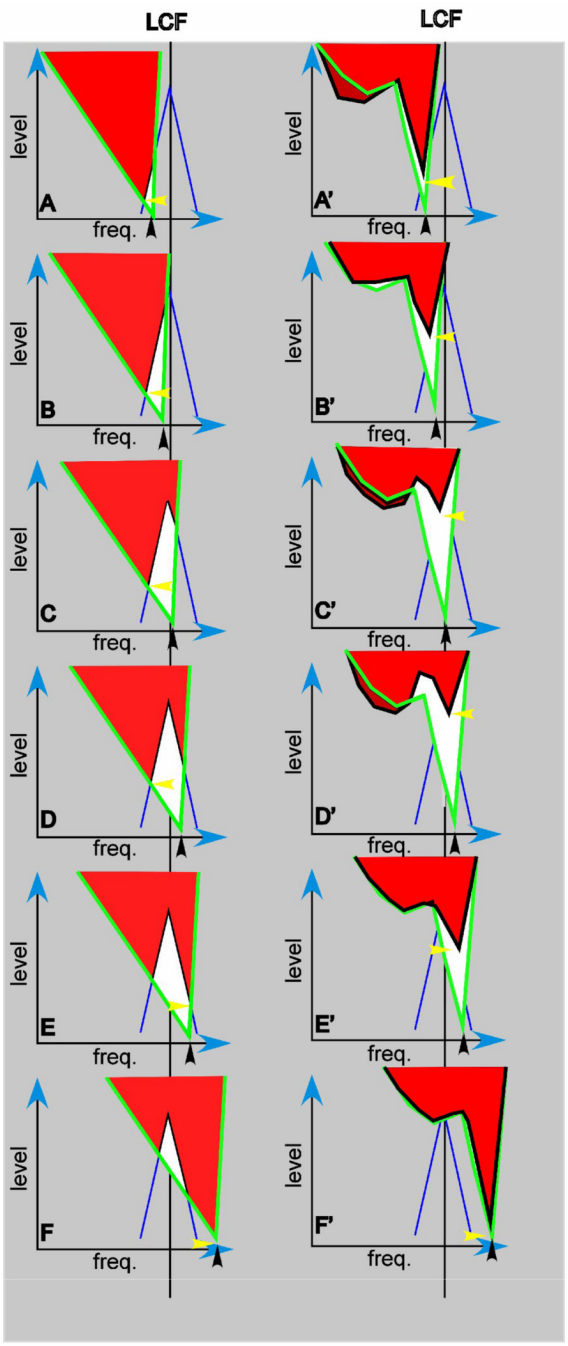

Figure 15.

Diagrammatic summaries of interactions between LCF and pre-lesion CFs of neurons in the ICC after a spiral ganglion lesion and in the auditory nerve after an acoustic tone lesion. Each panel in the left column represents pre-lesion and post-lesion tuning curve in ICC neuron observed before and after a spiral ganglion lesion. The post lesion curves are limited to those showing Type 1 response changes (losses of excitation [white areas] within the excitatory response area). Panels in the right column represent analogous responses in auditory nerve fibers observed before and after an acute acoustic lesion (based on Fig. 14, Liberman and Mulroy, 1982). LCF, the maximum CAP-threshold shift (vertical black line) and the width of sensitivity losses (blue lines) are the same in all 12 panels. In each pair of panels (A–A′ to F–

F′), the pre-lesion CFs (black arrows) shift in approximately equal steps from below (top) to above (bottom) LCF. Post-lesion CFs are indicated by the yellow arrows.) of auditory nerve fibers change relatively little from those observed prior to the acute acoustic lesion, whereas their thresholds shift dramatically. in some cases, auditory nerve thresholds are higher than the output of the stimulus system producing silent regions in the nerve (see Robertson, 1982). Note that the frequencies at which post-lesion notches (C′, D′) in the auditory nerve fiber responses occur are unrelated to LCF. In contrast, CF shifts between pre- and post-lesion responses in ICC neurons are relatively large. At progressive deeper (higher frequency) locations, post-lesion CFs change little in frequency (A–D) producing large pre-post CF differences until at a critical tipping point (between D & E) is reached. Above this point CF shifts dramatically from below LCF to above it and then follows the pre-lesion sequence. Post-lesion differences in ICC thresholds are relatively modest, compared to those observed in the auditory nerve and the notches are coincident with LCF.

Table 1

Post-lesion response type	Number	% Total	% of Changed
Type 0	40	36	
Type 1	30	27	43
Type 2	10	9	14
Type 3	6	5	9
Type 4	24	22	34
Total	110		